Energy 297 (2024) 131222

Contents lists available at ScienceDirect

Energy

journal homepage: www.elsevier.com/locate/energy

Review

Module defect detection and diagnosis for intelligent maintenance of solar photovoltaic plants: Techniques, systems and perspectives

Wuqin Tang [a,b], Qiang Yang [b,*], Zhou Dai [c], Wenjun Yan [b]

[a] Guizhou Key Laboratory of Intelligent Technology in Power System, College of Electrical Engineering, Guizhou University, Guiyang, 550025, China
[b] College of Electrical Engineering, Zhejiang University, Hangzhou 310027, China
[c] School of Management Science and Engineering, Guizhou University of Finance and Economics, Guiyang 550025, Guizhou Province, China

ARTICLE INFO

Handling editor: Soteris Kalogirou

Keywords:
Defect detection
Intelligent inspection
PV plants
EL and IR images
IoT technique and UAV-Based inspection

ABSTRACT

The energy production efficiency of photovoltaic (PV) systems can be degraded due to the complicated operating environment. Given the huge installed capacity of large-scale PV farms, intelligent operation and maintenance techniques and strategies are required to keep the healthy operation of the photovoltaic system. A complete inspection system, which is a key part of the intelligent operation and maintenance system, should focus on the following issues: defects types and mechanisms, defects detection methods, IoT techniques and UAV-based inspection methods. In this review, a comprehensive study is proposed to review and conclude the research advance and the prospects. In particular, given the complicated operation condition, we first review the environmental factor causing the defects and the corresponding possible degradation for PV modules. Then, the defect type and detection techniques are discussed and analyzed. Due to the strong ability for feature extraction, deep learning is a useful tool for defect detection of PV modules. Considering the location and geographical characteristics, conventional manual inspection is inefficient and even infeasible in practice. IoT techniques and UAV-based systems are utilized more and more popular, which are also discussed and summarized in this review. Due to the limit of the I/V sensors in the PV plants, this work reviewed the UAV-based system in detail, which has high efficiency for inspection and is widely used in industry, especially for visible and IR image-based systems. With technological advances in image sensors, the UAV-based system mounted with an Electroluminescence (EL) camera also presents huge potential. Finally, the conclusion and future direction for intelligent inspection and defect detection are provided.

1. Introduction

1.1. Motivation

In the past decade, due to the pursuit of low-carbon energy provision and technical advances in renewable energy, the installed capacity of solar photovoltaics (PV) has increased significantly. The statistics of the International Energy Agency [1] indicated that the global installed capacity of PV has reached 893 GW and the power generation has reached 1015 TWh by 2021. Following the trend, the operation and maintenance of PV plants have received huge attention in recent years for system safety, reliability and economic efficiency. Given the characteristics of PV plants, e.g., remote location and system complication, operation and maintenance have become a technique challenge. In reality, a PV power station is a complex system that contains various hardware and software units, such as an inverter and booster station on the AC side and photovoltaic modules on the DC side. Fig. 1 presents the statistics of defects in a typical solar photovoltaic power plant in Northwest China, and it indicates that the component with the largest failure rate (about 74 %) is the PV module on the DC side [2].

Since the large-scale PV plants are often located in remote areas with harsh operating conditions, e.g., lake surfaces and deserts, the PV modules are vulnerable to snow, dust and hail storms. The statistics in Ref. [3] indicate that 2 % of PV modules are predicted to defect about 10 years. Due to the tremendous number of PV modules in PV plants, failure can lead to significant economic loss and sincere failures can put safety risks for the plants. The process of converting solar energy into electric energy can be easily affected by external factors, such as solar radiation, mechanical stress and humidity. These factors can also influence the healthy operation of the PV modules. If these conditions are beyond a

* Corresponding author.
E-mail addresses: 11810073@zju.edu.cn (W. Tang), qyang@zju.edu.cn (Q. Yang), daizhou87@qq.com (Z. Dai), yanwenjun@zju.edu.cn (W. Yan).

https://doi.org/10.1016/j.energy.2024.131222
Received 24 October 2023; Received in revised form 15 March 2024; Accepted 5 April 2024
Available online 16 April 2024

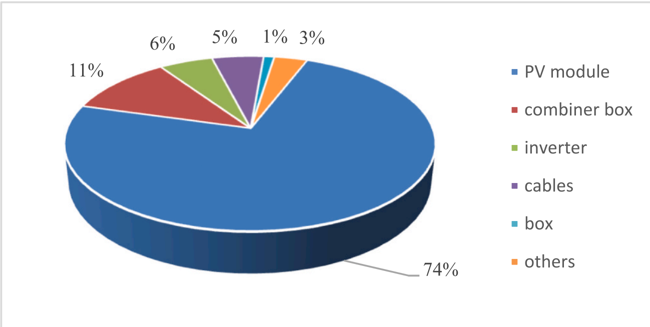

Fig. 1. Defects statistics of a photovoltaic power station in Northwest China.

certain range or last a long time, the degradation or defect, i.e., breakage, discoloration and corrosion, can appear. Existing studies have exploited and analyzed the impacts of environmental factors on PV module operation from different perspectives. To describe the defect detection issues for PV modules, it is important to conclude the impacts of the environmental factors. Moreover, a more specifically targeted inspection strategy or defect detection technique can be proposed based on the characteristics of the environment.

The rapid progress in artificial intelligence (AI) and the internet of things (IoT) techniques has improved the efficiency and accuracy of inspection greatly. At present, various research articles, which focus on the inspection of AI and IoT have been reported. Given the complexity of the inspection task, the techniques of AI and IoT can be divided into several types. The different deployment methods for IoT have different impacts on the inspection of PV modules. Nowadays, I/V sensors are widely deployed in plants to inspect the status of PV plants. However, due to the huge quantity, equipping an I/V sensor for each module will tremendously increase the cost, such as the installation and the post-operation and maintenance expenses. At present, the unmanned aerial vehicle (UAV)-based inspection system combined with IoT devices seems to be an effective solution for intelligent inspection, especially with the advances in communication, computing and robotics. For AI techniques, there are still some issues that need to be solved, e.g., the collection and annotation of the dataset, and computing efficiency.

Given the characteristics outlined above, the maintenance of solar plants is a complex and significant task. The rapid improvement of AI and IoT techniques has greatly changed the efficiency and features of the traditional. To illustrate the present state of research and prospects and provide a broad view of the maintenance techniques, this paper comprehensively reviews and analyzes the recent technical advances and latest research findings from different perspectives.

1.2. Literature review

At present, there are numerous publications focused on the defect detection of PV modules, and a substantial number of review articles are available that have focused on the operation and maintenance of PV plants (e.g., Refs. [3–18]). In Ref. [4], the categorization of detection and classification techniques were discussed and the defects were categorized based on visual, thermal and electrical methods. In Ref. [5], in addition to the introduction of the failures in PV modules, the relationship between the fire risk and hotspots was analyzed. As described above, the inverter is a key part of PV plants, the impact of the grid-connected PV inverter failures was discussed and the detection approaches were also concluded. In Ref. [6], the imaging techniques detection and a simple introduction to defect detection system were provided. In Refs. [7,8], image-based defect classification and detection were introduced and the characteristics of the aerial inspection systems were concluded. I–V was the most common defect detection technique for PV plants and the cell cracks (0.23) and hot-spots (0.18) were the most reported defects [9]. AI and IoT applied in the defect detection are analyzed in Ref. [10] and an IoT and AI-based smart configuration was suggested. The relationship between the monitoring system and fault detection technique and the defects detection was introduced and illustrated in Ref. [11]. Given the complex of the operation condition, the effect of the environmental factors on PV efficiency was discussed and the failure types are summarized in Ref. [12]. The prevention methods for fire in PV modules were introduced and evaluated in Ref. [13]. Due to the wide application of deep learning, artificial neural networks for defect detection are introduced in Ref. [14]. The monitoring system for PV plants is illustrated and analyzed in detail in Ref. [15]. In addition, working principles and evaluation techniques are presented for large-scale PV plants. Except for the failures and degradation mechanisms, the management strategies of the PV plants maintenance were presented in Ref. [16]. In Ref. [17], the typical defects detection after the inspection in North of Italy were described and the frequency data of the defects are provided. The definition of different defects was provided in Ref. [3]. Considering that IR imaging has been widely adopted, the patterns of the defects were illustrated.

In summary, the efficient and intelligent maintenance of PV plants receives increasing attention from the industry and much research effort has been made to design and develop the monitoring systems to improve the system maintenance performance. Thus, the timely summarization and discussion of the recent technical advances and practices as well as pointing out the future research directions can significantly benefit the development and maintenance of PV plants.

1.3. Contributions

The defects in the PV modules can be recognized by the electrical parameters (Current & Voltage, I/V) and images (e.g., visible, infrared thermography (IR) and luminescence). The electrical parameters analysis is a time-consuming technique to detect the defects, but it could have access to the PV module and it could increase the cost of the PV plants to establish access. The visible and IR image-based methods are non-contact techniques with high efficiency, while some defects cannot be recognized. The luminescence image-based techniques are contactless methods with high resolution, which can observe the inner status of the PV modules. However, the efficiency of the luminescence needed to be improved, especially for large-scale PV plants. Therefore, advanced sensing, AI and IoT technologies can be adopted in the operation and maintenance of PV plants to improve inspection efficiency and accuracy, it is necessary and valuable to review, analyze and conclude the related research.

This paper presents a critical review of the defect detection of PV modules for the maintenance of PV plants. The remainder of this work is organized as follows and illustrated in Fig. 2. Section 1 introduces the background and significance of defect detection for the PV module. Considering the complex operating environment, the factors that may cause defects are described and analyzed in Section 2. In Section 3, different types of module defect detection algorithmic solutions are presented and compared in detail. A promising solution for PV system inspection based on IoT and UAV technologies is presented and discussed. Finally, Section 5 concludes and presents the future work.

2. Overview of PV module degradation factors

The solar energy is converted into electrical power in PV cells which are the basic units of the module. The performance of PV modules can be affected by various factors, e.g., solar radiation, wind speed, temperature and the covering of the module surface. To some extent, the impact of a factor (e.g., temperature) could be offset by other factors (e.g., dust, wind). This section briefly discusses the main factors that can affect the power generation of PV modules.

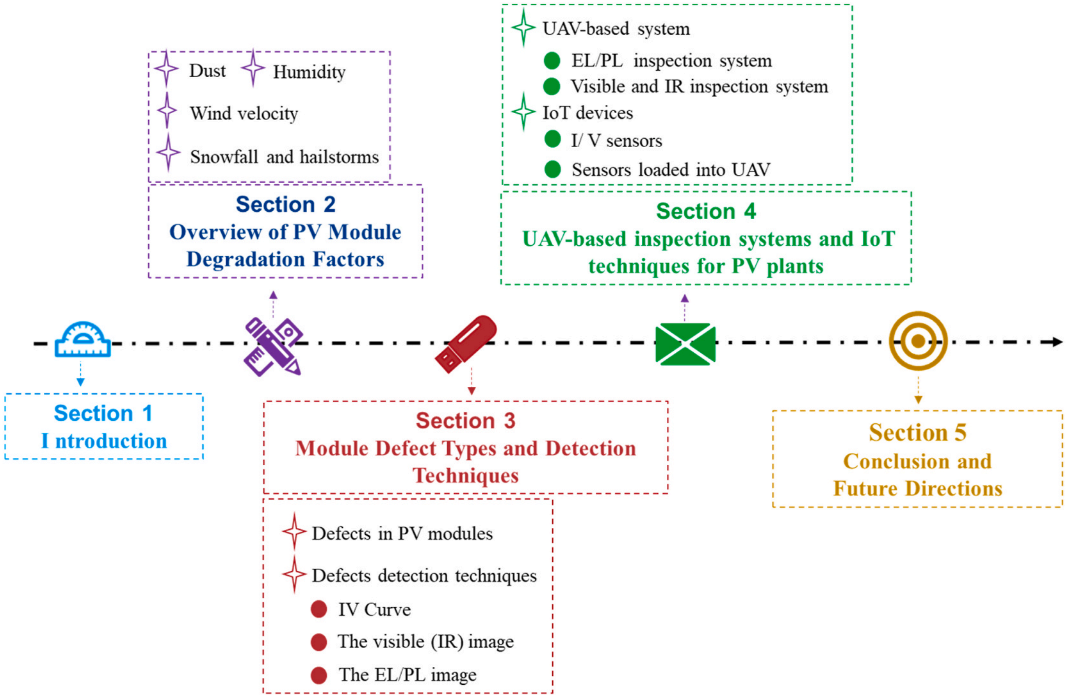

Fig. 2. Overview of the paper organization.

2.1. Dust covering impact

The shading due to dust, bird drops, and surrounding occlusion, covering the PV module surface can directly affect the energy conversion process of PV modules. Among these shading conditions, dust is a common shading condition that is mainly produced by environmental factors, e.g., rainfall, humidity and greening degree, in large-scale PV plants and may be hardly detected in practice. The dust in the distributed PV plants is mainly due to industrial pollutants and vehicle emissions [19].

Therefore, the degradation degree of PV modules in different locations can be different. In Ref. [20], the dust effect on the performance of the monocrystalline and polycrystalline modules with low-iron glass exteriors was investigated. Experiments have been carried out at the Birla Institute of Science and Technology (BITS)-Pilani, Hyderabad Campus, Hyderabad, India. The PV modules were exposed for 120 days without any manual cleaning and the results showed that the maximum power output dropped by 10.4 % and 4.32 % for monocrystalline and polycrystalline modules, respectively, with the natural dust accumulation. As the cleaning of dust can increase efficiency, a prediction model of the output power of PV modules was developed in Ref. [21] as given in (1):

$$\mathrm{Pt} = \varphi_0 + \sum\nolimits_{a=1}^{i} \varphi_a P_{t-a} + \varepsilon_t - \sum\nolimits_{a=1}^{i} \theta_a \varepsilon_{t-a} + \beta_k X_k \tag{1}$$

where φ, θ, β_k are the estimated parameters and X_k is the explanatory variables.

In [22], the dust pollution on PV modules mounted on the isolated building was investigated and the effect of various factors, e.g., dust particle sizes and gravity on dust deposition, was analyzed in detail. In addition, an empirical model was presented for the efficiency degradation ratios related to the exposure time. In Ref. [23], it was demonstrated that the dust deposition rates can be significantly increased along with the increased wind velocity. In Ref. [24], the power generation loss was measured by the experiments for 120 days at an open rooftop in Lahore. The results showed that the optimal cleaning schedule for the modules at 30°and 90°is about once a week and three weeks, respectively. A novel model of energy conversion efficiency was proposed [25] and the impacts of wind, particle flow as well as dust deposition on the PV modules were investigated. The degradation of conversion efficiency can be enhanced with the increase of the dust particle diameter and wind speed and the higher the deposition time is, the lower the efficiency is. When the deposition time is 100, the efficiency can drop to 11.3 %. The maximum loss of the conversion efficiency can reach 72.9 % at high wind speed. In Ref. [26], an approach is proposed to investigate the efficiency of dust and temperature to PV modules in a hot and arid area and it is noticed in this paper that the high temperature and dust can greatly decrease the highly suitable areas for PV plants, which can decrease by 81 % in the serious condition. The efficiency of PV plants in some areas, e.g., Kathmandu, which has an abundant deposition of dust with less rainfall, could be easily affected and permanent damage to the module could occur due to the dust accumulation. A regression equation for calculating the power loss caused by the dust is built in Ref. [27]. This work also presented an experimental result that compared with the module daily cleaned, the efficiency of the module with natural dust deposition dropped by 29.76 %. In east China, the main components of dust are SiO_2 and C_aCO_3. The work in Ref. [28] proposed a PV equivalent model and a prediction model. To collect the PV power generation, a meteorological and electrical data collection system was built and the system has operated for two years. Compared with the cleaned modules, the power outputted by the module covered by dust dropped by 7.4 % in the week of dust deposition. The effects of the dust were analyzed and listed in Table 1. It can be concluded that dust could reduce the efficiency of PV modules and other factors, e.g., wind or tilt angle of the modules can relieve the degradation caused by dust.

2.2. Temperature impact

The efficiency of Si-based PV modules is sensitive to temperature, which plays a key role in the process of power generation of PV modules. The low or high temperature in the PV plants could decrease the efficiency of energy conversion. The effects of temperature can be evaluated using (2), as suggested in Ref. [35].

$$P_{\mathrm{m}} = V_m I_{\mathrm{m}} = FF \times V_{OC} I_{SC} \tag{2}$$

When the temperature increases, the V_{OC} and I_{SC} decrease. To

Table 1
PV generation degradation due to dust.

Ref.	Methods	Duration	Location	Maximum degradation
[20]	Experiment	120 days	India	10.4 % (monocrystalline) 4.32 % (polycrystalline)
[21]	Model	–	–	–
[22]	Model	–	–	–
[24]	Experiment	120 days	Lahore	–
[25]	Model and Experiment	100	–	11.3 %
[26]	Model	–	Hot arid area	81 %
[27]	Model and experiment	–	Kathmandu	29.76 %
[28]	Model and experiment	a week	East China	7.4 %
[29]	Experiment	Weekly, monthly, 2 months, and 7 months	Palestine	9.99 %
[30]	Experiment	15 weeks	United Arab Emirates	Transmittance of 30 %
[31]	Experiment	A month	North of Oman	50 %
[32]	Experiment	–	Iran's desert environment	98.2 % (dark shading conditions)
[33]	Model	–	Tenerife	–
[34]	Experiment	100 days	Pakistan	13 %–26 %

investigate the profiles of temperature and power output, a novel model was proposed in Ref. [36]. The model analyzes the effects of wind on power output and the effects of the profiles of temperature on the heat loss coefficient from a PV. In Ref. [37], a thermal model is developed to predict the performance of PV modules and the performance of PV plants located in Ankara, Turkey is analyzed with a heat capacity value. In addition, the results of the proposed model are invariant with different capacity values. In Ref. [38], a mathematical model for the coupled thermal and electrical performance of the PV module was formulated to identify the relationship between the thermal and electrical performance in detail. The root means square error (RMSE) and means bias error (MBE) values of the output on a winter day are 5.094 W and −0.022 %, which are 3.913 W and −2.499 % in summer, respectively. The relationship between the radiative thermal resistance and the temperature is also illustrated, which is 80.3 % and 70.7 % on winter and summer days. By the simulation techniques in Ref. [39], in Kuwait, the power generation in spring is 13 % higher than in summer, when the temperature and climate are milder and the maximum power generation can be obtained. In contrast, the power generation stability in summer is higher than in winter. The variability of the power generation of power in summer is the same. The sensitivity of the PV modules with amorphous silicon and monocrystalline silicon for temperature is different, which is demonstrated in the experiment [40].

In addition, the system loss for amorphous silicon and monocrystalline silicon was 5~6 % and 3–4 % in the experiment, respectively. The efficiency of PV systems can be degraded by about 0.5 %/K [41]. The dust and water in the humid air conditions could create mud. The surface cover with the high temperature can significantly reduce the generation efficiency of PV modules and the reduction can reach about 25 % under the condition of high drying temperatures [42]. Due to the efficiency variation caused by temperature, the gap between the panels and the rooftop can influence the temperature of PV modules and the function of the gap is analyzed in Ref. [43]. The efficiency of PV panels in STC is 18.04 %, but it is reduced to 14.17 %, 15.01 % and 15.44 % when the gap becomes 0 mm, 200 mm and 250 mm, respectively. In Ref. [44], the cooling method is utilized to lower the temperature. 11.69 % electrical efficiency can be obtained for the PV system when water and air cooling are used.

2.3. Wind velocity impact

The direct impact of wind on PV module efficiency is relatively small. However, the wind can carry dust or particles in or out of the PV modules and the temperature can also be influenced. The temperature can be calculated using (3) [45]:

$$T_c = f(T_a, V, G_s, material, \ldots) \tag{3}$$

where T_a is ambient temperature, V presents wind velocity and G_s is solar irradiance. The energy conversion can be calculated based on (4):

$$\eta = \eta_{Tref}\left[1 - \beta_{Tref}\left(T_c - T_{ref}\right)\right] \tag{4}$$

where η_{Tref} is the electrical efficiency of the PV module under the reference temperature and 1000 W/m^2. The β_{Tref} is the parameter related to the material of the PV module.

In [46], the cooling effect of the wind speed for the PV modules is presented by a simulation method. The wind speed can make the modules much cooler. In addition, the yearly energy output could be higher by 3.5 % in the simulation, when the wind speed is considered. The floating PV system has a lower work temperature and higher efficiency than the land-based PV system [47]. The study in Ref. [47] demonstrated that when the working temperature decreases by 11.6 %, the output of power can increase by about 20.28 % and the electrical efficiency can increase by 32.82 % when the wind speed increases by 49 %.

2.4. Humidity impact

The humidity can change the distribution of solar radiation toward the PV modules and the temperature, which plays a key role in the energy conversion process. To some extent, the increment of humidity, and the temperature of the module surface could be reduced, which could increase the power output. However, the increment also decreases the radiation at the same time [48]. In the experiments performed on [48], the humidity level is set as 65.40 %, 70.20 %, 73.50 %, 76.40 %, 80.40 %, 85.60 %, 91.70 %, 95.10 % and 98.20 %. The corresponding radiation for the PV modules are 854, 823, 802, 784, 759, 726, 688, 667 and 648 (W/m^2), and the corresponding temperatures are 39.5, 39.1, 38.6, 38.3, 38.1, 37.4, 36.9, 36.3 and 35.0 (°C). The corresponding output power (W) of the PV modules is 7.84, 7.38, 7.13, 6.90, 6.48, 6.04, 5.60, 5.37, and 5.00. It can be observed that the output power was reduced by 36.22 % due to the increment of 50.15 % of the relative humidity. The relative humidity on the surface of PV modules can be approximated by the following equation [49]:

$$SRH = 100 \times \left[\frac{Exp\left(\frac{17.625\times T_d}{234.04+T_d}\right)}{Exp\left(\frac{17.625\times T_m}{234.04+T_m}\right)}\right] \tag{5}$$

where T_d is the dew point temperature and T_m is the module temperature.

In practice, the impact of potential induced degradation (PID) can be evaluated by the leakage current. The effects of the humidity and temperature on leakage current are analyzed in Ref. [50] and it has been observed in the experiments that the leakage current increases when the value of the humidity increase. In addition, high voltage is the major reason for PID and relative humidity is the second factor. The Prandtl number and the thermal conductivity between the air and module can be influenced by humidity [51]. The performed experiments confirmed that the increase in humidity can make the temperature of the module surface higher. In this paper, a differential equation is established and solved to illustrate the relationship between temperature and humidity. It is concluded that humidity can influence the temperature, which can impose a significant impact on the output power of the PV modules. The service lifetime prediction and evaluation are critical and difficult, which can also be affected by variables, e.g., temperature and humidity. To accurately predict the uncertainties in degradation rates and service lifetime, three factors of uncertainties are analyzed and discussed [52]. The highest uncertainties in degradation rates (1.7 %–14.5 %) are caused by temperatures and the second is caused by relative humidity (2.4 %–12.2 %). However, this conclusion could be different in other locations. The equivalent circuit of the PV cells is utilized to analyze the humidity effects in Ref. [53]. It was concluded that the inception of moisture can lead to significant degradation in the maximum power generation and the short circuit current of the PV cells. The result in Ref. [54] indicated that the current was reduced by 44.44 % with the relative humidity increment from 67 % to 95 %.

2.5. Snowfall and hailstorms impact

Some PV plants located in cold areas, e.g., northwest China, may often face severe degradation caused by snowfall and hailstorms. Snow and ice covered on the surface of PV modules can greatly reduce the obtained solar irradiation and the surface temperature. In addition, the hailstorms could damage the module surface. PV plants can be considered a financial investment due to their characteristics. However, the study in Ref. [55] showed that when the system life of the plants is between 25 and 50 years, the return on investment could be reduced by 0.56 %–0.50 % due to the potential degradation of the modules caused by snowfall. The monthly and annual electricity loss caused by snow is less than 10 % in the common climate in general, but the monthly loss could reach higher than 25 % in winter [56]. The effects of snow have a strong relationship with climatic patterns and plant system characteristics. It is reported that rain and snow have the most negative impacts on the performance of PV modules and when the weather is snowing or rainy, the power output of the PV modules could be 0 [57]. In Ref. [58], the effect of snow on six PV systems, which are 2 residential systems, 2 small commercial systems, a 100 kW PV system on the roof and a 200 kW with ground-mounted racks, are analyzed and discussed in Colorado and Wisconsin during the winter of 2010~2012. The monthly output loss can reach 90 % and the annual loss ranges from 1 % to 12 %. Given the tilt angles can also influence the effects caused by snow, the PV modules with 4 tilt angles (0°, 15°, 30° and 45°) in Calumet, USA, are utilized to measure the output loss caused by snow [58]. The experimental platform was inspected and evaluated for 1 year in Oct. 2013. For the elevated unobstructed modules, the annual loss ranges from 5 % to 12 % and the least loss is obtained for the modules with the steepest tilt. The annual loss of the obstructed modules ranges from 29 % to 34 % and the tilt has little impact on the loss. The annual power loss of the PV modules with the different tilt angles (0°–15°), which are located in the snowiest urban areas in the U.S., ranges from 12 % to 18 %. However, the monthly loss is much higher than the annual and the monthly loss of the PV modules with little tilt angles could be 100 % when the depth of snow reaches several feet [59].

The hails with different severity can create different damages for PV modules. In the worst condition, the modules can be broken and even a fire can be caused. Given the characteristics of the defects, some techniques, e.g., electricity data, thermography, electroluminescence (EL) and UV-fluorescence imaging, are utilized to evaluate the negative impact caused by hails [60]. In the experiments, the efficiency and output of three PV plants were inspected and analyzed with non-destructive defect detection techniques in July 2015. Before and after the hailstorm, only one plant presents the obvious degradation in monitoring data on the system level, when the damaged modules are replaced. It is also reported that the damages caused by hailstorms cannot be detected easily with thermography. However, the damages can be recognized by EL and UV-F imaging and the power measurements demonstrate that the invisible damages can result in about 30 % power loss.

3. Module defect types and detection techniques

3.1. PV module defects

Unlike the defects on the AC side, which can be easily detected by electrical data, the defects in PV modules are more difficult to recognize, especially the tiny defects in PV modules [61]. As presented in Fig. 1, the PV modules have the highest defect rate in a plant. The reason, characteristics and impact for different defects could be various. Table 2 presents the reason, energy loss, and characteristics of different typical module defects [5,62].

3.2. Defects detection techniques

The effect of the different techniques, especially for the data-driven methods, depends on the measuring method, data collection and the embedded defects information. Due to the difference in mechanism, different defect detection methods have different application scenarios. This section presents the characteristics of commonly used defect detection techniques in the publications and a brief conclusion and

Table 2
Summary of the defects in PV modules.

Defects	Energy loss	Reasons	Defects characteristic	Detection techniques
Crack	1 % ~15 %	Subjected mechanical stress or loads	Cracks in the PV modules	EL, PL
Shading	10 % ~40 %	Something partial or entire covering the module	Surface of PV module covered	Visible image or naked eyes
Soiling	10 % ~30 %	Soil, dust or snowfall on the surface	The soiling accumulation on the surface	Visible image or naked eyes
Hotspot	2 % ~20 %	Inner defects or shading	Higher temperature than around areas	IR
Pid	10 % ~70 %	Stray currents in ungrounded systems	Negative voltage or positive voltage to ground	Negative voltage or positive voltage
Snail track	1 %~8 %	The materials and processing of the modules	Snail track form on the surface module	Visible image or naked eyes
Frame breakage	–	Snowfall or severe hails storm	Modules frame damaged	Visible image or naked eyes
Corrosion of cell busbars	1 % ~15 %	The moisture penetration in the high temperature or humidity condition	Color changes around the busbars	EL, PL and visible images
Failure bypass diode	33 %	Inner short circuit, open circuit or other damages in the diode or junction box	Hotspot in IR images	IR and visible images
Discoloration	1 % ~30 %	Humidity, high temperature or others bad climate conditions	discoloration on the surface of modules	Visible images
Finger failure	–	Subjected mechanical stress or loads	Thin region around the finger in the cells	EL, PL
Overheating junction box	1 % ~33 %	Inner damage of the junction box	High region in the IR images	IR

comparison are provided.

3.2.1. IV curve

The idea behind the defect detection by I/V is that the electrical parameters could be changed before and after the defects. Various publications recommend that the I/V curve is a cost-effective, easy and reliable operation [9]. I/V curve can reflect important electrical parameters, such as the short-circuit current (I_{sc}), open-circuit voltage (V_{oc}), and fill-factor (*FF*). The defects, that caused the obvious changes in electrical data, such as short circuit (SC), open circuit (OC) and shading, can be accurately detected. Based on [63], defect detection with I/V is a relatively complete technique and the critical part of it is the data acquisition system, which can obtain the electrical data and other environmental factors. Therefore, the variation caused by defects can be examined by I/V. However, some defects, which only cause tiny variations in the electrical parameters, is uneasy to detect by the I/V measurements [64] and the defects cannot be accurately located at the module level in the PV plants [65].

The advances in deep learning and computer science have brought huge improvements in the defect detection of PV modules. Due to their strong ability in data analysis and processing, artificial neural networks (ANN) are widely used to analyze electrical data. Given the difficulty of the data collection, simulated electrical parameters are utilized for defect detection, but the performance of the models trained with the simulated data could be decreased in real conditions. In some publications, the electrical data with 1 dimension are directly transferred into the defect detection models [63–75] and given the high feature extraction ability of ANN, the series of electrical signals are converted into 2D images (2 dimensions) before transferred into the models in other publications [76–82].

The characteristics and results of the publications for defect detection with electrical data are listed in Table 3. It can be observed that the average accuracy obtained by the data-driven defect detection methods is much higher than 90 %, which is more excellent than the traditional data analysis technique. However, the simulation data is widely used by data-driven techniques, which could be different from the real operation parameters and could reduce the performance in the field. Therefore, data acquisition is a challenge for the application of the data-driven methods and given the numerous quantities, it could be a huge expense to equip an I/V sensor for each PV module in the plants. In conclusion, unless an I/V sensor for each module, the electric parameters-based methods cannot locate the defect at the module level and some tiny defects cannot be recognized. Therefore, even though the electric parameters can directly reflect the output of the plants, there are still some issues to limit the application.

3.2.2. Visible/infrared (IR) image-based techniques

The visible image-based method is a non-destructive and low-cost method for defect detection. Several defects, e.g., cracks, yellowing, dust shading, gridline corrosion, breakage and snail trails, can be directly observed and recognized by the visible images [80,81]. Discoloration is a common defect for PV modules, especially for a plant located in the desert. The statistics in Ref. [82] indicated that encapsulant discoloration occurred for all 608 modules located in Algeria. The defects, yellowing and browning can cause the primary power loss in the whole PV system [84–86]. Defect detection with the naked eye is a typical application of visible image-based methods. It is well known that defect detection with the naked eye cannot meet the current demand for inspection for large-scale PV plants, especially for large-scale plants [87,88]. The conventional methods with IR images also meet the same challenges. Based on the results in Ref. [89], the human-based inspection of a 3 MW PV plant (in total of 17142 modules) needs to take 34 days and another 26 days are required to analyze and process the collected images. IR image-based methods are another non-destructive defect detection. The idea behind it is that the defect areas of PV modules have a higher temperature than the defect-free and emit more IR radiation, which can be captured by the specified IR camera. Given the imaging principle and defect characteristics, the visible and infrared cameras are integrated and loaded into the unmanned aerial vehicle (UAV) to increase efficiency. Due to the strong ability to process images, ANN is also employed to analyze the collected images.

Many types of module defects can be recognized by the IR and visible images. Several typical defects in visible or IR images are illustrated in Table 4 ([88,90,91]). It is obvious that the defects definition in IR images mainly depends on the shape or location of the hotspot. However, given the low resolution, keeping a high accuracy for defect detection with IR images is uneasy, especially for similar defects. The same defect presents different characteristics in the IR and visible images. Compared

Table 3
Defects detection techniques with electrical data.

Ref.	Method	Data source	Input	Detected defects	Average accuracy
[66]	Data-driven	Simulation	I/V curve (plane)	PID, SC, OC	98.5 %.
[67]	Traditional data analysis	Field	I/V measurement	PID	–
[68]	Traditional data analysis	Field	I/V data	Partial shading, hot spot, crack	95.7 %
[69]	Traditional data analysis	Field	I/V data	Crack	–
[70]	Data-driven	Simulation and field	Key points of the measured I/V curve	Degradation, short-circuit fault, partial shading	98.6 % (simulation data) and 91.4 % (field data)
[71]	Data-driven	Simulation and field	Corrected and sampled I/V curve	Defected	100 %
[72]	Data-driven	Simulation and field	I/V curve	Partial shading, short-circuit, degradation, open-circuit	97.3 % (simulation data) and 98.3 % (field data)
[73]	Traditional data analysis	Experiments	Dark I–V characteristics	PID	–
[74]	Traditional data analysis	Experiments	voltage at maximum power (V_{mp}) and the current at maximum power (I_{mp})	Shading	–
[75]	Data-driven	Experiments	temperature, peak voltage, peak current	Crack, short circuit and the shading	90 %
[76]	Data-driven	Simulation	2-Dimension electrical time series graph (current and voltage)	Open-circuit line-line fault	99 %
[77]	Data-driven	Simulation	The grayscale image (converted from current and voltage)	Line-ground, line-line and partial shading	99.70 % (grid-connected modes) and 98.86 % (islanding modes)
[78]	Data-driven	Simulation and experiments	Current-voltage curve, irradiance and temperature	Short-circuit faults, open circuit faults, degradation faults, and partial shading	Higher than 92.31 %
[79]	Data-driven	Experiments	IV curves	Partial soiling, and cracked	99 %
[83]	Data-driven	Experiments	IV curves	Defected	99.4 %

Table 4
Patterns of different PV defects in visible and IR images.

Defects	Description	Assessable method	Examples (defected modules)
Defect-free	No obvious warmer area	–	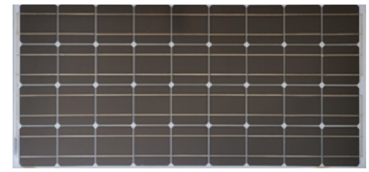
Modules in open Circuit	The modules do not connect to the grid and one module is warmer than the others	IR images	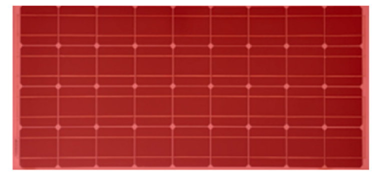
Short circuit, substring open circuit	In a module, one or two rows warmer than others	IR images	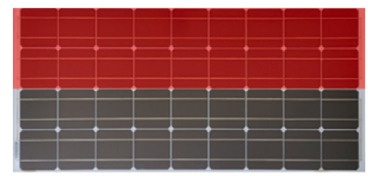
Bypass diode or short circuit	Some cells in a module are warmer than others	IR images	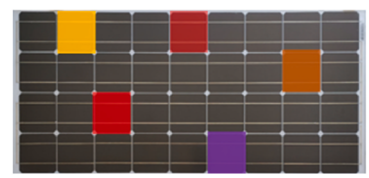
Massive shunts	Some cells and the cell near the frame are warmer than the rest of the modules	IR images	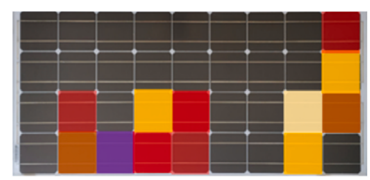
Defected cell, shading or delaminated cell	One cell is warmer than others in the module	IR and visible images	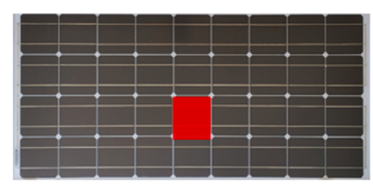
Shading	Unregular areas are warmer than others in a module	IR and visible images	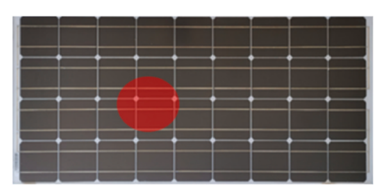
Breakage	Part of one or more cells are warmer than others	IR and visible images	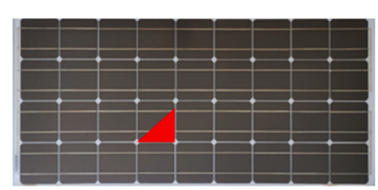

(*continued on next page*)

Table 4 (*continued*)

Defects	Description	Assessable method	Examples (defected modules)
Overheating junction box	The junction box is warmer than other areas	IR images	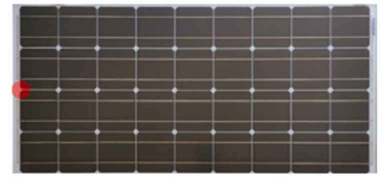
Ethylene vinyl acetate falls off	One of the encapsulant delamination	The visible	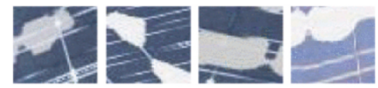
Dust shading	Dust accumulation on the surface of the module	The visible and IR (hotspot) image	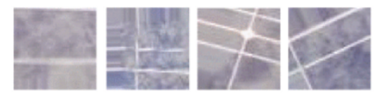
Glass breakage	The glass on the module surface has been broken	The visible and IR (hotspot) image	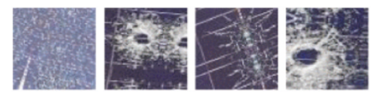
Snail trails	The feature of the defect appears like a small dark line on the module surface	The visible image	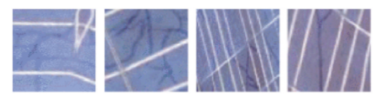
Yellowing	Color of partial modules changes into yellow or brown	The visible image	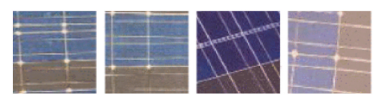

with IR images, visible images carry more detailed defect information for recognition. The defects on the surface of PV modules can be easily detected and classified. However, the inner faults cannot be recognized by the visible.

At present, due to the superior performance in the image process and recognition, ANN is widely adopted for defect detection of PV modules based on IR and visible images. A modified pre-trained VGG16 is trained with the IR images collected from both far and close-distance and the classification accuracy of 0.98 is obtained in Ref. [92] for 3 types of PV modules. To improve the performance, U-Net and a classifier, which uses the decision tree, are combined to detect the defects in Ref. [93]. The defect features extracted by U-Net can significantly improve the performance of defect detection. The complex background can create huge noise for defect detection with IR images. Two-stage algorithms are developed to overcome the problems in Ref. [94]. In the first stage, the PV arrays are extracted from the complicated scene and then the PV module in the array is extracted and classified and the experimental results prove the efficiency and accuracy of the solution. To relieve the limit of the dataset size, transfer learning is adopted to recognize the defects in Ref. [95] and the experimental results confirmed that the accuracy obtained is 0.5 % higher than the isolated learned technique. A huge aerial dataset of IR images is established in Ref. [96]. To improve the performance, transfer learning is also introduced and a mean accuracy of 94.88 % is obtained. Support vector machine (SVM), which has higher computing efficiency than deep learning, was utilized for defects detection with IR in Ref. [97] and the hotspot can be detected with high accuracy. In Ref. [98], 8 types of PV modules with IR images were analyzed and discussed to evaluate their performance under different conditions, under-sampling and over-sampling are compared and the results illustrate that the over-sampling can improve the generalization of the proposed CNN-based model. A novel attention module was integrated into CNN (RCAG) for the task of defect detection with IR images in Ref. [99] and the experimental results show that some small hot spots can be recognized with the proposed algorithm.

Based on the defect information carried by the visible images, soiling and partial shading are assessed with the deep learning-based technique [100]. The power loss can also be quantified in this work. An accuracy beyond 70 % for 4 types of classification tasks is obtained with a small size of the visible image dataset in Ref. [101]. To improve the performance, the PV modules are also extracted by semantic segmentation and classified. In the inspection process, it is unavoidable to meet the unknown or unlabeled dataset types of PV modules. To address or relieve the limits, an unknown online defect detection system is established in Ref. [102], which combines transfer learning, data augmentation and an opportunistic speedup unit. The high performance of the proposed solution is demonstrated by numerous experiments. A three-stage algorithm is proposed in Ref. [2] to increase efficiency and accuracy. Given the characteristics of the defects, the Kirsch operator is used to crop the anomalous areas and then, a CNN is employed to extract the defect features. Finally, SVM is utilized to classify the defects. In Ref. [103], a CNN-based model is proposed to classify the 5 types of defects.

As mentioned above, the visible images contain detailed PV module surface information and the IR can provide the defect information. The fusion of the IR and visible images can make the best use of the information for defect detection. Therefore, the IR and visible images are combined to analyze the defects in some studies [104–107]. In Ref. [104], a novel framework, which combines the YOLOv5 and ResNet models, is proposed to segment and identify the defects. The IR and visible images are captured at the same shooting angle and height. The IR images are utilized to segment and identify the PV module and the defects. The defects are located with visible images. To increase the efficiency, a UAV mounted with IR and a visible camera is built in Ref. [105]. YOLOv3 is also introduced to detect defects. In addition, the accuracy and efficiency of the proposed framework are proved in the two PV plants in Italy. Based on [106], hotspots are the most common defects and are always caused by soiling and vegetation.

The details of the mentioned techniques are concluded in Tables 5 and 6 out of 15 cases in Table 5 have obtained detection accuracy higher than 95 %. Except for the defect classification, the segmentation for locating the defects is also applied in 3 references, which can provide the

Table 5
Defects detection techniques with the IR and visible images.

Ref.	model	Input (image)	Dataset size			Accuracy	Defects types
			Train	Validate	Test		
[92]	Pretrained VGG16	IR images collected from far and near-distance	200 hotspots, 200 hot substrings, and 716 health modules			98 %	Hotspots; hot substrings;
[93]	U-Net + Decision tree	IR images collected with FLUKE Ti450	1852	–	500	99.8 % for classification; 95.2 % for segmentation	Safety-glass cracks; PV power unit defects; pollution of safety-glass
[94]	Modified U-Net	IR images with the UAV (camera FLIR Vue Pro)	1211			95.71 % for classification; 99.79 % for segmentation	Hotspots
[95]	Light CNN	IR images	893			99.23 %	Defective
[96]	Modified VGG16	Aerial IR images	83,898		9322	94.88 %	One hotspot; patchwork pattern of hotspots; overheated module row; overheated module; pointed heating
[97]	Support vector machine (SVM)	IR images	315 PV modules			92 %	Hotspot (65–80 °C); faulty (above 80 °C)
[98]	CNN	IR images	14,450	2250	3000	92.5 % for defects and 78.85 % for the 8 types	Diode and connection Loss; cell or Multiple cells; soiling; cracking; hot Spot and multiple Hot-spots; partial shading; offline Module
[99]	CNN + Attention Network	Aerial IR images	790	–	4270	84.64 %	Hot spot
[100]	Mask RCNN + ANN	the visible images	19,200	4800	–	73 %	Soiling and partial shading (based on the power loss)
[101]	CNN (semantic segmentation + classification)	Aerial visible images	345 images			75 % for 2 output classes and 70 % for 4 classes	Cracks; shadows; dust
[102]	CNN (transfer learning + clustering)	Aerial visible images	5000			99.6 %	Dust shading; glass breakage; gridline corrosion; Snail trails; yellowing
[2]	CNN + SVM	Aerial visible images	–			0.972	Dust shading; glass breakage; gridline corrosion; snail trails; yellowing
[103]	CNN	Aerial visible images	5880	1680	840	98.7 %	Dust shading; glass breakage; gridline corrosion; snail trails; yellowing
[104]	YOLOv5+ RestNet	The visible and IR images	2200	700	100	91.7 % in segmentation and 95 % in defect detection.	Hotspot
[105]	YOLOv3	The visible and IR images	1426 (IR) 1050 (Vis.)		306 (IR) 225 (Vis.)	98.91 %	Hotspot; strong soiling; raised_panel; soiling; puddle; bird_dropping
[106]	–	The visible and IR images	–			–	Hotspot Soiling Vegetation breakage
[108]	RGR-Net	The IR images	–			89.8 %	Hotspot
[109]	CNN + SVM	The visible and IR images	–			97.52 %	Dirt vegetation snail hot cell open Circuit cell crack DC box component
[110]	YOLOv5	The visible and IR images	800	0	200	87.8 %	Hotspot
[111]	traditional methods	The visible	–	–	–	–	Hotspot

Table 6
Comparison among the defects detection systems [112].

Metrics	Grounded-based system (multi-camera)	Grounded-based system (single-camera)	UAV-based system
Latency	High	High	Low
Efficiency	Low	Low	High
Cost	High	High	Low
Security	Low	Low	High
Image quality	High	Low	High
Reliability	Low	Low	High

precise location of the defects. At present, due to the advances in UAV techniques, visible and IR images are frequently applied in the industry. The aerial technique can greatly improve efficiency and reduce cost, especially for large-scale PV plants. The IR image contains the temperature information of the module surface and the visible image carries the surface information. Some defects, based on the location of the hotspot, can be accurately identified in IR images. However, due to the low resolution of the IR image, the hotspot location in the PV module cannot be always obtained. Compared with the IR image, the visible has a higher resolution and most defects in the visible images can cause a hotspot. Some studies combined the IR and visible images for accurate identification and diagnosis of the module defects. Given the characteristic of the images and the related reference, a reliable and accurate method is that the hotspot area in the IR images is first detected, and then the corresponding area of the hotspot area in visible images are classified further, which can increase the accuracy of defect detection. The advantages of the technique are the low cost, high efficiency and easy operation and the main limit is that the relatively poor embedded defect information and some inner defects cannot be observed or identified with the visible and IR images. It indicates that the IR and visible image-based techniques could not meet the demand for precise inspection.

3.2.3. The EL/PL image-based techniques

Electroluminescence (EL) and photoluminescence (PL) images can provide the inner perspective to evaluate the state of the PV module with the different imaging principles. EL and PL images have more detailed fault information than IR and visible images. The idea behind the EL and PL is that the material of the PV module can emit electromagnetic radiation after being activated by the irradiation and a specified electrical current, respectively [7]. The emitted radiation can be captured by a specified camera. For defect detection, EL can provide more detailed information about the electrical function of the module, while PL contains more information about the material quality of the module. Therefore, the information both in EL and PL can also be utilized to identify the defects from a different perspective.

The defect detection with EL images is briefly illustrated in Fig. 3. A complete inspection system contains a specified camera (image collection), a portable power supply (providing the current) and a computer (image process). Given the principle of EL imaging, inspection is always performed at night to decrease the disturbance of the noise [107]. Based on the specifications in Ref. [113], the signal-to-noise (SNR) needs to be higher than 5 in the process of the inspection. With the increase in power conversion techniques, the activated current can be automatically injected with the bi-directional inverter, which is directly connected to the PV modules [114,112]. The massive application of the inverters can tremendously increase inspection efficiency and can make EL inspection a real contactless method. At present, the EL inspection can be divided into 2 types: ground-based and UAV-based, which are illustrated in Fig. 4 (a), (b) and (c) [112], respectively. In the ground-based system, a multi-camera could be used to improve the efficiency, as shown in Fig. 4 (a). However, there are always some PV plants that are not suitable for the multi-camera system and a single-camera system is proposed to address the issue, as shown in Fig. 4 (b). The UAV-based system, as presented in Fig. 4 (c), can obtain the highest accuracy. Moreover, given the endurance time of the UAV, the camera mounted in the UAV is always lighter than the ground-based system and the image resolution could be lower than the image collected in the ground-based system. With the technological advances in cameras and UAVs, the resolution difference between the two systems can be eliminated or relieved. The comparison of the three systems is presented in Table 6 [112].

To perform the daylight inspection with EL, several techniques, such as using optical filters and image processing, are proposed in Refs. [115–117]. The noise in the background can be greatly filtered by optical filters and image processing techniques. Although adequate information existed in the images, there is no clear definition for the defects in EL images. The common defects collected with the ground-based and UAV-based systems are present in Fig. 5, respectively [118–120]. In the image, the gray value of the pixel is related to the photoelectric conversion capability and the mean intensity of the cell image reflects the output power [121]. The image intensity is also proportional to the activated voltage level. Therefore, when the activated voltage level is fixed, the defected areas should be darker than the good condition.

Given more embedded adequate information on the defects, much research effort has been made on the module defect detection with the EL images. Similar to defect detection with IR/visible images, ANN is also widely applied for defect identification with EL images and excellent performance is obtained. Before transferring into the ANN-based model, several methods, such as distortion correction, are used to preprocess the collected images. Based on the structure of the PV module, the defects at the cell level and module level are all discussed and analyzed in studies. In addition, different techniques, such as defect classification and segmentation, are utilized for different purposes. The details of the defect detection techniques with the EL images are listed in Table 7. Here, three studies adopted the UAV-based system for defect detection with EL images and the other 15 references used the ground-based system. At present, the ground-based system is the mainstream approach, but the UAV-based system has great potential due to its high efficiency. It can be observed that different performances are obtained with the different techniques and datasets. Deep learning-based has huge advantages over other techniques. Based on the statistics, the mean accuracy in 14 out of 16 references is higher than 85 % and two public datasets are provided in Refs. [122,123]. It can be observed that 8 out of 16 references and 1 out of 16 references used the public dataset provided in Refs. [122,123] to train or evaluate the proposed approach. The detected defect types are different in different references. The results in Table 7 are also presented in Fig. 6.

Similar to the EL imaging technique, photoluminescence (PL) imaging can also be performed in daylight and the difference between the techniques is the activated source. The noise caused by the sunlight reflection can greatly affect the PL image qualification. To reduce the impact of the sunlight, a specified PL camera is always loaded with a bandpass filter [142]. In addition, due to the state of the PV module in daylight, the inspected module needs to be switched between the open circuit and the short circuit. Compared with EL, PL performed in daylight is activated by the sunlight and does not need an additional

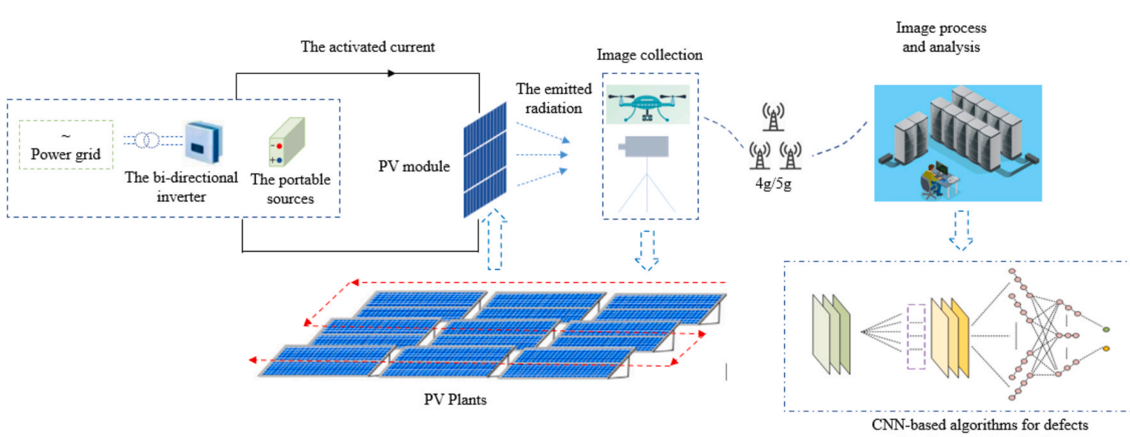

Fig. 3. Defect detection system with EL images.

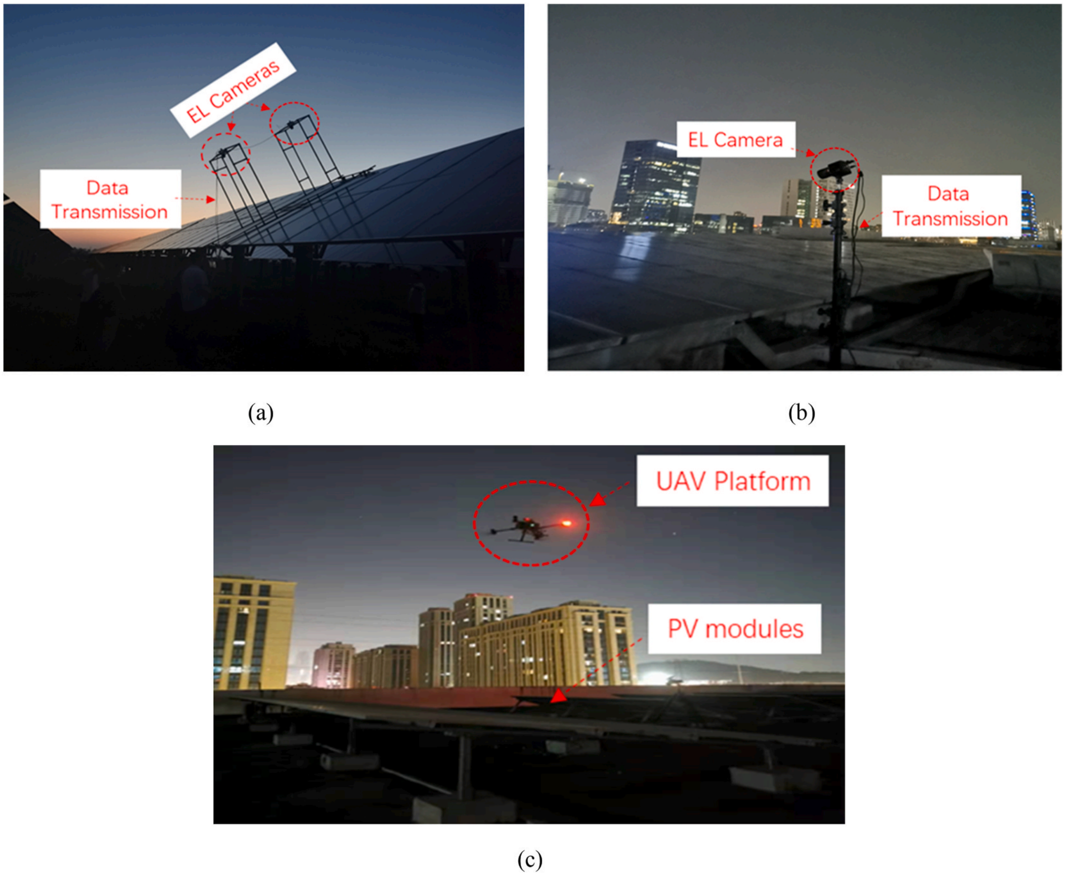

Fig. 4. Different types of system implementation for EL inspection: (a) the ground-based system with multi-camera; (b) the ground-based system with single-camera; (c) UAV-based system [112].

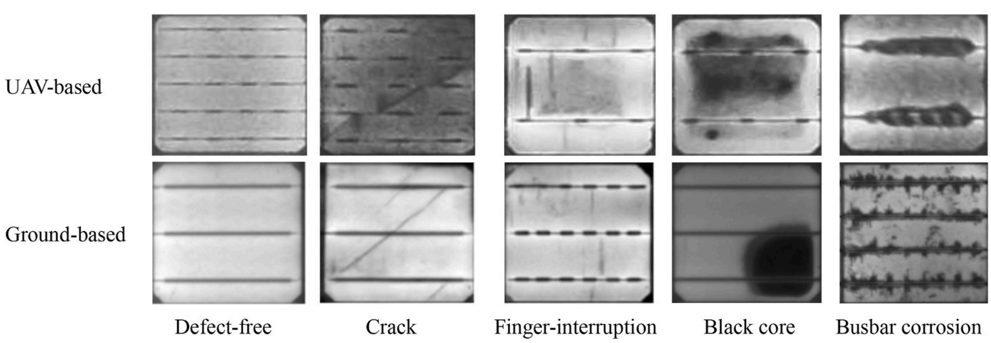

Fig. 5. Different types of defects in EL images.

power source to activate. However, the switch of the PV module is another important limit for the application of the PL. To address the above-mentioned limit, the LED lamp or high-powered laser is utilized to illuminate the module with a shorter wavelength that does not disturb the PL imaging process. Given that the illumination caused by LED or laser is weakened than the sunlight, the PL imaging process can be performed under light or dark conditions to improve the quality of the images. The process of PL imaging is illustrated in Fig. 7.

Given the relatively small illumination area of the point or line laser, imaging a complete PV module could take a long time. It will put a high demand for the flight stability and endurance of the UAV system. In addition, the laser equipment can bring about an additional safety threat to the UAV. The study in Ref. [143] demonstrated the setup can impose a significant impact on the application of UAVs. The illumination caused by the point or line laser can cause a huge voltage difference between the illuminated and unilluminated areas, as shown in Fig. 8 [143–145]. The illuminated areas can be enlarged by replacing the laser with LED arrays, which are lighter, smaller and safer. The LED can cover several cells simultaneously and is a better choice for application in the UAV-based system.

The imaging qualities based on EL and PL techniques are different in different conditions. The comparison between the two techniques is discussed and analyzed in Ref. [146] and the images collected in different conditions are presented in Fig. 9 [146]. The difference between the indoor and outdoor EL images is little and the partially isolated or unfunctional areas are presented in EL images that cannot be observed in the PL images.

Table 7
the defect detection techniques with the EL image.

Ref.	Algorithms	Input sources	Dataset	Defect level	Purpose	Dataset size			Defect types	Mean accuracy
						Train	Val.	Test		
[114]	Traditional + CNN	Ground-based	Public [122]+ private	Cell	Classification + segmentation	4200	400	800	Linear defect	93 %
[112]	Traditional + CNN	UAV-based	Private	Cell	Classification	1200		400	Crack busbar corrosion cell degradation	97.9 %
[118]	CNN + clustering	UAV-based	Private	Cell	Classification	3500	1000	500	Crack finger-interruption, black core, busbar corrosion	96 %
[119]	CNN	Ground-based	Public [122]+ private	Cell	Classification	1200		400	Micro-crack, finger-interruption, break	83 %
[120]	CNN	Ground-based	Public [122]	Cell	Classification	2624			Defective	93 %
[124]	U-net	Ground-based	Public [122]+ private	Cell	Segmentation	–		30	Inactive, crack, gridline	68.7 %
[125]	CNN	Ground-based	Public [123]	Cell	Classification	2841	711	889	5 types of busbar, corrosion	95 %
[126]	Imaging process + electrical model	Ground-based	Private	Cell	Classification	–			Defective	98.90 %
[127]	Multi-channel CNN	Ground-based	Private	Module	Detection	861	–	600	Break, crack, unsoldered area	98.3 %
[128]	Modified U-net	Ground-based	Private	Cell	Segmentation	620	–	208	Crack, finger-interruption	0.699(IoU)
[129]	YOLOv4+light CNN	Ground-based	Private	Cell	Detection	600	–	120	Crack, dirty	99.36 %
[130]	CNN	Ground-based	Private + public [122]	Cell	Classification + segmentation	4512	1080	–	Defective	99.36 %
[131]	Machine learning + CNN	Ground-based	Public [122]	Cell	Classification	–			4 types of defectives (based on the defect possibility)	90.57 %, 94.52 % for 4 and 2 class
[132]	CNN	Ground-based	Private	Cell	Classification	2840	–	710	Corroded, crack	99 %
[122]	CNN	Ground-based	Public	Cell	Classification	2281	–	646	4 types of defectives (based on the defect possibility)	88.42 %
[133]	Traditional image processing	Ground-based	Private	Cell	Detection	–	–	–	Crack	–
[134]	Fuzzy CNN	Ground-based	Public [122]	Cell	Classification	2099	–	525	4 types of defectives (based on the defect possibility)	88.38 %
[135]	Traditional image process + CNN	UAV-based	Private	Cell	Classification	400	100	100	Linear defect	93 %
[136]	DeepLabv3+	Ground-based	Private + public	Cell	Segmentation	80,000			Crack gridline inactive ribbons spacing	/
[137]	CNN	Ground-based	Public	Cell	Classification	9856			Black core crack finger dislocation material short circuit thick line	96.06 %
[138]	Traditional image process + CNN	Ground-based	Public	Cell	Classification	1968	/	656	Defected	90.55 %
[139]	CNN	Ground-based	Private + public	Cell	Classification	1970	/	654	Defected	91.74 %/94.26 %
[140]	Yolov8	Ground-based	Public	Cell	Object detection	4530			/	92.6 %
[141]	CNN	Ground-based	Public	Cell	Classification	720	–	210	Micro-cracks	90.15 %

3.3. Comparison among the defect detection methods

As mentioned above, the different defect detection methods for PV modules have different characteristics. It is obvious that defect detection with I/V is a low-cost and effective method and the power loss can be directly and accurately detected. Compared with the vision-based method, a sincere problem is that the defect cannot be located and some tiny defects can also be not recognized. For the vision-based method, the combination of the IR and visible images has excellent efficiency, low cost and easy operation, but the embedded defect information in the images is less than in EL and PL images. It means that the IR and visible can be used regularly for inspection and if more details information about the defects is needed, EL and PL image-based techniques could be a better choice. A comparison of these methods in detail is presented in Table 8.

4. UAV-based inspection systems and IoT techniques for PV plants

The internet of things technique (IoT) is a framework that integrates numerous devices, such as sensors and actuators to inspect and control the industrial system. During the past few years, IoT has been discussed and applied for the inspection and monitoring of PV plants and numerous benefits can be achieved by employing the IoT such as high

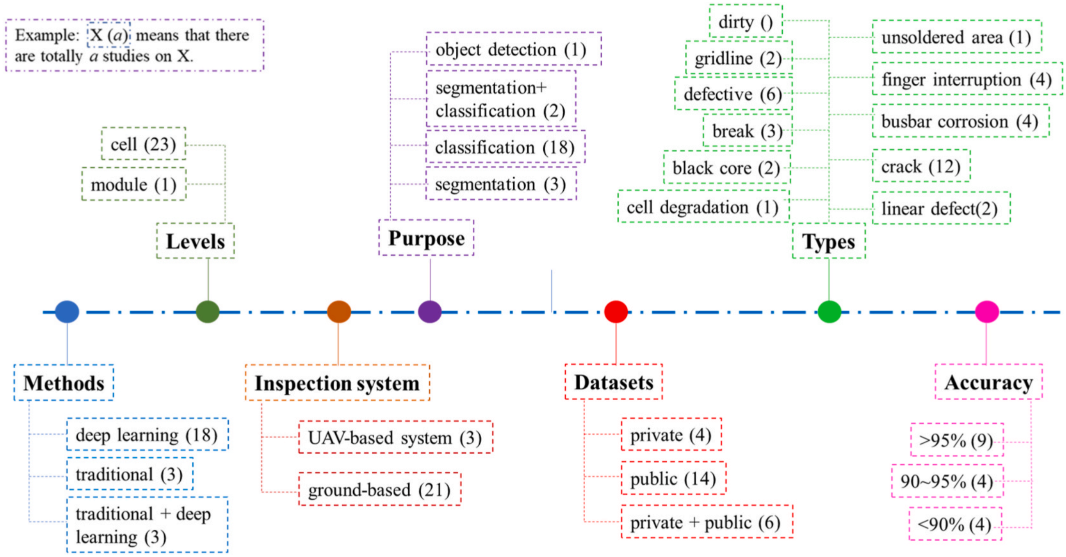

Fig. 6. Statistical analysis of the solutions presented in Table 7.

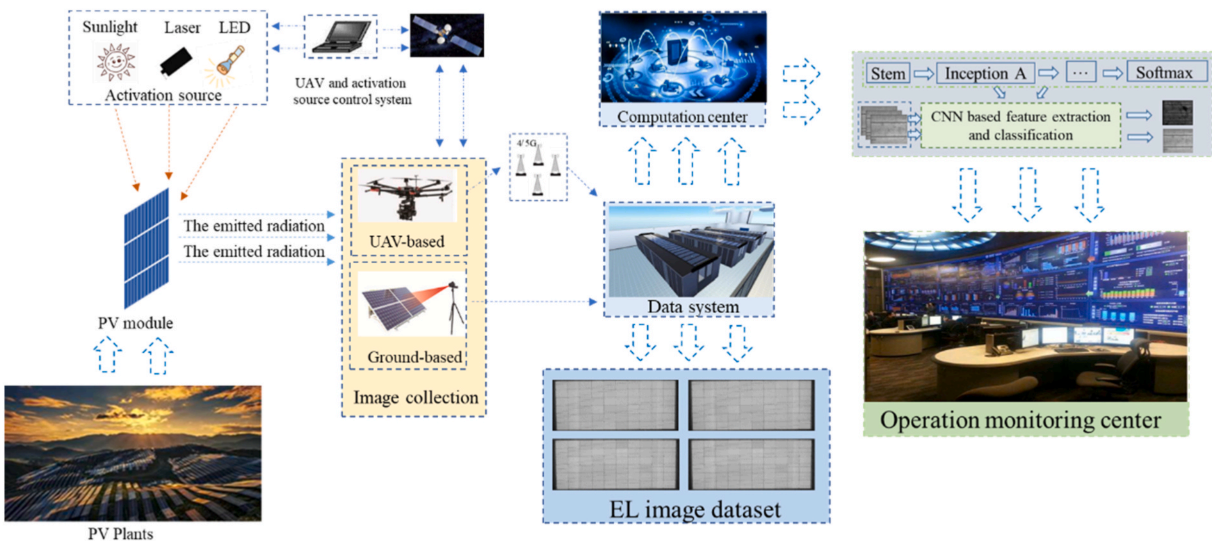

Fig. 7. PL imaging and analysis process.

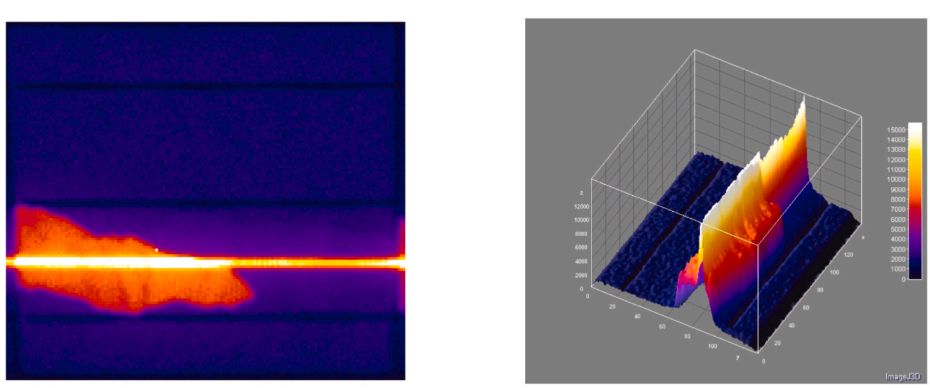

(a) (b)

Fig. 8. PL images illuminated by the line laser (a) the PL image; (b) the corresponding numerical distribution in 3D [145].

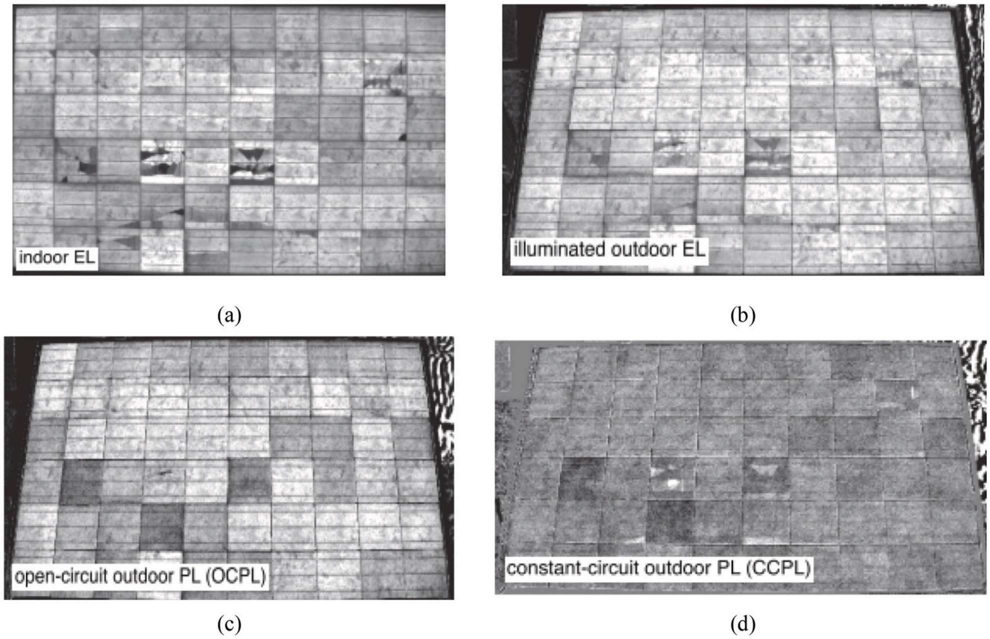

Fig. 9. Images in different conditions: (a) indoor EL; (b) outdoor EL; (c) open-circuit outdoor EL; (d) constant-circuit outdoor PL [146].

Table 8
Comparison of the different defect detection methods.

Specifications	I/V	Visible	IR	EL	PL
Wavelength of the imaging signal	–	Visible	1400–7000 nm	1400–7000 nm	1400–7000 nm
Equipment	I/V sensors	Visible cameral	IR camera	EL camera and power source for illumination	PL camera and illumination source (laser, LED or sunlight)
Operation condition	Normal	Normal	Satisfying minimum irradiation intensity	Low light or dark	Low light or dark
Advantages	Low cost, easy collection and quantitative evaluation	Quick, low cost and non-intrusive	Quick, defect locating and non-intrusive	Accurate, reliable, high-resolution, cell-level defects locating	Non- intrusive, high-resolution, accurate
Disadvantages	Cannot identify the defect location and several tiny defects	Cannot identify the invisible defects	Relatively low resolution and little defect information	Requiring additional power source and low efficiency	Requiring additional excitation source and low efficiency

efficiency, accuracy and a reduction of economic costs. Given the characteristics of the UAV, the combination of the IoT and UAV can greatly increase the benefits. In this section, the inspection system with UAVs is mainly introduced and analyzed.

Different forms of IoT devices, e.g., GPS (Global Positioning System), were utilized to inspect the electrical parameters state of the PV plants [147,148]. However, some defects cannot be accurately recognized by the electrical parameters. In addition, the cost of installation and operation can greatly increase when too many devices are deployed in the plants. Therefore, more data acquisition techniques, e.g., IR, EL and PL images, are required to perform an accurate evaluation of the PV plants. The IR, EL and PL cameras can be mounted on the UAV as IoT devices to get more detailed defect information. The applications of remotely piloted aircraft loaded with IR cameras for PV plant inspection are summarized and reviewed in Ref. [149]. Compared with the traditional methods, the inspection can be reduced by 10–15 times. During the inspection process, obtaining the accurate location of the UAV and the corresponding inspected modules is important. The view of the camera loaded is mainly determined by the UAV position and all inspected PV modules should be captured by the camera with high precision to ensure the inspection quality. In Ref. [150], the Real Time Kinematic (RTK) was integrated into the UAV to increase the positioning accuracy and the experiments proved that the application of RTK can provide an effective field of view in 97 % of cases, which is more accurate than GPS. In Ref. [151], an integrated software package (RoboPV) is proposed for the automatic inspection and monitoring of PV plants with UAV, which mainly contains four parts: boundary area detection, path planning, dynamic processing and fault detection. The package provides a basic pipeline for the automatic inspection of PV plants with a UAV mounted with a visible camera. Given the characteristics of RoboPV, the inspection with IR can also be supported.

To ensure the inspection of all PV modules with high efficiency and low costs (time and energy consumption), the areas of interest in the field of view are identified during the inspection with UAV in Ref. [152]. The flight parameters during the inspection (e.g., height, waypoints, inspection path and view angles) are optimized by the genetic algorithms and the particle swarm optimization. For the UAV-based system loaded with an IR camera, the camera settings (e.g., the speed of the UAV and the height) can directly affect the image quality. Several factors, such as the relationship between incidence angle and emissivity, can also degrade the defect detection performance with IR images. Given the principle of imaging, the incidence angle and emissivity can also influence defect detection with EL and PL images. A series of algorithms are proposed in Ref. [153] to correct the map of IR during the post-process, which can correct the image acquisition and ensure the correct reading of IR images. In Refs. [2,102,103], UAV-based systems with visible cameras for condition monitoring and maintenance of large-scale PV plants were developed and different algorithms were integrated into the systems for different inspection purposes. To reduce the response time, edge devices and communication units are also equipped in the UAV. In Refs. [112,118], the UAV-based system with an EL camera is introduced for the inspection of PV plants. Given that an additional power source is required for illumination, the system with an EL camera is more complicated than the system with a visible camera. In addition, the demand for a positioning system in the EL inspection system is higher.

The details of the mentioned studies with UAV-based systems for inspection are summarized in Table 9 and to illustrate the structure of the UAV-based system, the typical systems are presented in Fig. 10 [2, 112]. As mentioned above, several devices or units are equipped to keep the safe, steady and efficient operation of the inspection system. GPS or RTK is required to position the UAV and PV panels. As presented in Ref. [150], RTK is more precise than GPS at a more expensive price. Given the complicated conditions in the PV plants, a flight control system should be integrated into the UAV, which can be embedded into the onboard processor, such as the Manifold. In addition, different cameras are mounted for different purposes. In conclusion, the inspection systems with visible or IR cameras are relatively mature compared to the techniques with EL or PL cameras. Given the defect information embedded in the image, the UAV-based system with an EL or PL camera has great potential. With the development of processors and UAVs, the steady online detection or inspection system has profound significance.

5. Conclusion and future directions

Due to the rapid development and increasing capacity of PV generation infrastructures across the world, the safe operation and efficient maintenance of PV plants have received increasing attention from both research and engineering communities. However, the power generation of PV plants is directly related to several environmental factors, e.g., irradiance and temperature. In practice, it is hard to find a place where the environmental factors are all suitable for the operation of PV plants. Therefore, Understanding the relationship between environmental factors and power generation, as well as defects, and the prevalent detection methods is crucial for the development of the PV industry. Through the review and analysis of the existing studies, the following key findings can be observed.

(1) Considering that the occurrence of extreme weather events, e.g., hail, sand storms and floods, become more frequent, the effects of typical environmental factors and their interactions on PV plants are analyzed and discussed.
(2) Due to the variations in detection methodologies and recognition criteria, the characterization of PV defects and the extent of their hazards is complicated. The typical defects descriptions are provided and the possible power loss generated by the defects is presented.
(3) Because of the improvement of AI techniques, vision-based and I/V-based methods are utilized to detect the defects. The advantages and disadvantages of the defect detection methods are compared, analyzed and concluded.
(4) Given that the IoT and UAV can hugely increase efficiency, the application of IoT and UAV for PV plant inspection is also introduced. The statistics in the studies show that the UAV mounted with multi-sensors is more efficient than the traditional I/V sensors, but the traditional methods can directly reflect the performance of the PV modules.

The research directions worth further effort are summarized as follows.

(1) The inspection and defect detection decision-making: The occurrence probability of the defects needs to be calculated and analyzed based on the operation statistics of the PV plants. Several specified defect detection techniques should be applied based on the weather and climate conditions. The customized inspection and defect detection strategy can decrease the cost and increase defect detection accuracy.
(2) The precise locating of the defection: the defect information obtained during the inspection needs to be integrated with the

Table 9
Summary of the UAV-based systems.

Ref.	Function	Devices	Inspection image	Detection level	Defect detection	Online detection
[150]	Accurate positioning	IR camera; Pixhawk 2.1 Cube; RTK system	IR	PV module; PV array	No	No
[151]	Path planning; image collection; defect detection	Pixhawk 4; Holybro autopilot; Nikon 1-V1 RGB camera	Visible	PV module; PV array	Yes	Yes
[152]	Path planning; view angles; waypoints	IR camera	IR	PV module; PV array	No	No
[153]	Correcting the parameters during inspection (the emissivity, the reflected temperature, and the resolution)	IR camera	IR	PV module; PV array	No	No
[102]	Online data collection and processing;	DJI Matrix100; DJI manifold; LightBridge2; Visible camera	Visible	PV module; PV array	Yes	Yes
[2]	Online data collection and processing;	DJI Matrix100; DJI manifold; LightBridge2; Visible camera	Visible	PV module; PV array	Yes	Yes
[103]	Online data collection and processing;	DJI Matrix100; DJI manifold; LightBridge2; Visible camera	Visible	PV module; PV array	Yes	Yes
[112]	Online data collection and processing;	DJI Matrix300; DJI manifold2; EL camera	EL	PV module and cell	Yes	Yes
[118]	Online data collection and processing;	DJI Matrix300; DJI manifold2; EL camera	EL	PV module and cell	Yes	Yes

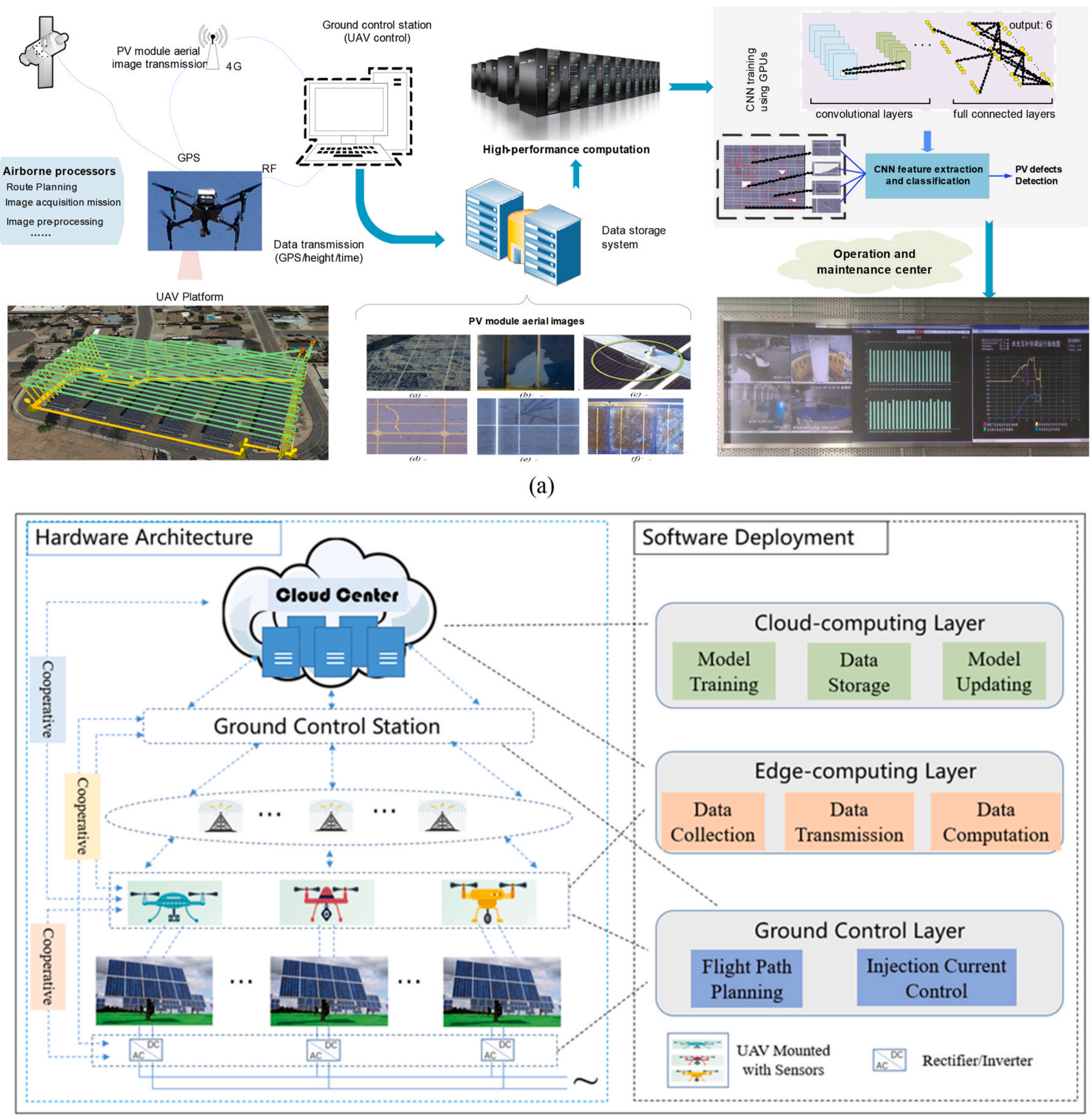

Fig. 10. Typical UAV-based system for inspection of PV plants. (a) the UAV-based system mounted with a CCD camera; and (b) the UAV-based system mounted with EL image sensors [2,112].

position information of the corresponding PV modules or arrays. It means that more precise techniques, e.g., the RTK, cloud point image and PV module segmentation techniques, are acquired to get the position of each module in PV plants.

(3) The defects information combination: the relationship between the different images (IR, visible, EL and PL) and the I/V should be obtained by numerous experiments. If the defect information in images can be translated into electric information, the PV module evaluation could be more efficient and reliable. The combination of I/V sensors and UAV-based systems can provide a more cost-effective solution for the precise health evaluation of PV plants and an intelligent module-level inspection system solution is required, as suggested in Fig. 11.

(4) The existing defect detection solutions can only detect one type of defect in an image. In fact, there are always multiple types of defects that exist in an image and prior knowledge should be introduced for defect detection, which could relieve the limit of the data size for deep learning.

(5) Emerging IoT and AI-based algorithms can significantly improve the efficiency of the inspection system, especially when the IoT and AI algorithms are loaded or embedded into the UAV.

(6) Given the cost of data collection, defect detection solutions based on few available samples need to be further exploited in future work and the corporation of multi UAV can also increase the efficiency of inspection.

CRediT authorship contribution statement

Wuqin Tang: Investigation, Methodology, Validation, Writing – original draft. **Qiang Yang:** Conceptualization, Funding acquisition, Supervision, Writing – review & editing. **Zhou Dai:** Funding acquisition, Visualization. **Wenjun Yan:** Validation, Writing – review & editing.

Declaration of competing interest

The authors declare that they have no known competing financial interests or personal relationships that could have appeared to influence

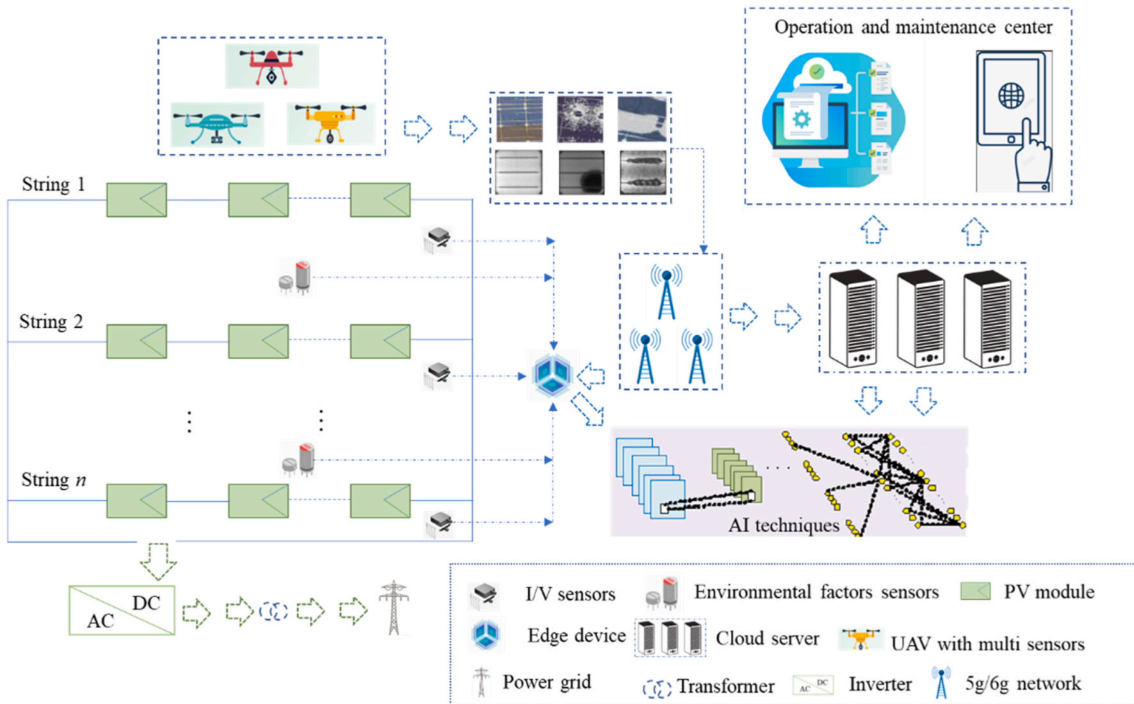

Fig. 11. Suggested UAV-based inspection system for PV modules.

the work reported in this paper.

Data availability

No data was used for the research described in the article.

Acknowledgment

This work is supported by the Special Support Plan for Zhejiang Province High-level Talents (2022R52012), the National Natural Science Foundation of China (52177119) and the Evaluation and Early Warning Innovation Team for Quality in Electric Power Equipment Manufacturing of Guizhou Province's Higher Education Institutions (QJJ[2023] 064).

References

[1] IEA. Renewables 2021 data Explorer. Paris: IEA; 2021. https://www.iea.org/articles/renewables-2021-data-explorer.
[2] Li X, Li W, Yang Q, et al. An unmanned inspection system for multiple defects detection in photovoltaic plants. IEEE J Photovoltaics 2020;10(2):568–76. March.
[3] Review of failures of photovoltaic modules final: Tech. rep. Report IEA-PVPS T13-01:2014.
[4] Hong Y, Pula RA. Methods of photovoltaic fault detection and classification: a review. Energy Rep 2022;8:5898–929.
[5] Waqar M, Li G, Jin Y. Failures of photovoltaic modules and their detection: a review. Appl Energy 2022;313:118822.
[6] Malik A, Haqu A, Kurukuru VS, et al. Overview of fault detection approaches for grid connected photovoltaic inverters. e-Prime-Advances in Electrical Engineering, Electronics and Energy 2022:100035.
[7] Høiaas I I, Grujic K, Imenes A, et al. Inspection and condition monitoring of large-scale photovoltaic power plants: a review of imaging technologies. Renew Sustain Energy Rev 2022;161:112353.
[8] Yahya Z, Imane S, Hicham H, et al. Applied imagery pattern recognition for photovoltaic modules' inspection: a review on methods, challenges and future development. Sustain Energy Technol Assessments 2022;52:102071.
[9] Rahman M, Khan I, Alameh K. Potential measurement techniques for photovoltaic module failure diagnosis: a review. Renew Sustain Energy Rev 2021;151:111532.
[10] Mellit A, Kalogirou S. Artificial intelligence and internet of things to improve efficacy of diagnosis and remote sensing of solar photovoltaic systems: challenges, recommendations and future directions. Renew Sustain Energy Rev 2021;143:110889.
[11] Madeti Siva Ramakrishna, Singh SN. A comprehensive study on different types of faults and detection techniques for solar photovoltaic system. Sol Energy 2017;158:161–85.
[12] Santhakumari Manju, Sagar Netramani. A review of the environmental factors degrading the performance of silicon wafer-based photovoltaic modules: failure detection methods and essential mitigation techniques. Renew Sustain Energy Rev 2019;110:83–100.
[13] Wu Zuyu, et al. A review for solar panel fire accident prevention in large-scale PV applications. IEEE Access 2020;8:132466–80.
[14] Li Baojie, et al. Application of Artificial Neural Networks to photovoltaic fault detection and diagnosis: a review. Renew Sustain Energy Rev 2021;138:110512.
[15] Madeti Siva Ramakrishna, Singh SN. Monitoring system for photovoltaic plants: a review. Renew Sustain Energy Rev 2017;67:1180–207.
[16] Gonzalo Alfredo Peinado, Pliego Marugán Alberto, et al. Survey of maintenance management for photovoltaic power systems. Renew Sustain Energy Rev 2020;134:110347.
[17] Grimaccia Francesco. Survey on PV modules' common faults after an O&M flight extensive campaign over different plants in Italy. IEEE J Photovoltaics 2017;7(3):810–6.
[18] Kandeal AW. Infrared thermography-based condition monitoring of solar photovoltaic systems: a mini review of recent advances. Sol Energy 2021;223:33–43.
[19] Zarei Tahereh, Abdolzadeh M, et al. Comparing the impact of climate on dust accumulation and power generation of PV modules: a comprehensive review. Energy for Sustainable Development 2022;66:238–70.
[20] Enaganti Prasanth K. Experimental investigations for dust build-up on low-iron glass exterior and its effects on the performance of solar PV systems. Energy 2022;239:122213.
[21] Kennedy Joel. Solar and sand: dust deposit mitigation in the desert for PV arrays. Sustainable Energy, Grids and Networks 2021;28:100531.
[22] Hao L, Lu L, Wang Y. Numerical investigation of dust pollution on a solar photovoltaic (PV) system mounted on an isolated building. Appl Energy 2016;180:27–36.
[23] Hao L. Numerical study on poly dispersed dust pollution process on solar photovoltaic panels mounted on a building roof. Energy Proc 2019;158:879–84.
[24] Ullah Asad. Investigation of soiling effects, dust chemistry and optimum cleaning schedule for PV modules in Lahore, Pakistan. Renew Energy 2020;150:456–68.
[25] Fan Siyuan. A novel model to determine the relationship between dust concentration and energy conversion efficiency of photovoltaic (PV) panels. Energy 2022;252:123927.
[26] Charabi Yassine, Gastli A. Integration of temperature and dust effects in siting large PV power plant in hot arid area. Renew Energy 2013;57:635–44.
[27] Paudyal B, Shakya Raj SR. Dust accumulation effects on efficiency of solar PV modules for off grid purpose: a case study of Kathmandu. Sol Energy 2016;135:103–10.
[28] Chen Jinxin. Study on impacts of dust accumulation and rainfall on PV power reduction in East China. Energy 2020;194:116915.

[29] Juaidi Adel. Experimental validation of dust impact on-grid connected PV system performance in Palestine: an energy nexus perspective. Energy Nexus 2022;6:100082.
[30] Dhaouadi Rached. A characterization study for the properties of dust particles collected on photovoltaic (PV) panels in Sharjah, United Arab Emirates. Renew Energy 2021;171:133–40.
[31] Kazem A Hussein, Miqdam T. The effect of dust accumulation and cleaning methods on PV panels' outcomes based on an experimental study of six locations in Northern Oman. Sol Energy 2019;187:30–8.
[32] Sadat Seyyed Ali. The experimental analysis of dust deposition effect on solar photovoltaic panels in Iran's desert environment. Sustain Energy Technol Assessments 2021;47:101542.
[33] Cañadillas-Ramallo David. The influence of extreme dust events in the current and future 100% renewable power scenarios in Tenerife. Renew Energy 2022;184:948–59.
[34] Ullah Asad. Investigation of optimal tilt angles and effects of soiling on PV energy production in Pakistan. Renew Energy 2019;139:830–43.
[35] Manju S, Sagar N. A review of the environmental factors degrading the performance of silicon wafer-based photovoltaic modules: failure detection methods and essential mitigation techniques. Renew Sustain Energy Rev 2019;110:83–100.
[36] Kaplanis S, Kaplani E, Kaldellis JK. PV temperature and performance prediction in free-standing, BIPV and BAPV incorporating the effect of temperature and inclination on the heat transfer coefficients and the impact of wind, efficiency and ageing. Renew Energy 2022;181:235–49.
[37] Tuncel B. Dynamic thermal modelling of PV performance and effect of heat capacity on the module temperature. Case Stud Therm Eng 2020;22:100754.
[38] Yaman Kaan, Arslan G. A detailed mathematical model and experimental validation for coupled thermal and electrical performance of a photovoltaic (PV) module. Appl Therm Eng 2021;195:117224.
[39] Alshawaf Mohammad, Poudineh R, et al. Solar PV in Kuwait: the effect of ambient temperature and sandstorms on output variability and uncertainty. Renew Sustain Energy Rev 2020;134:110346.
[40] Maftah A, Maaroufi M. Experimental evaluation of temperature effect of two different PV Systems Performances under arid climate. Energy Proc 2019;157:701–8.
[41] Machniewicz Anna, Knera Dominika, et al. Effect of transition temperature on efficiency of PV/PCM panels. Energy Proc 2015;78:1684–9.
[42] Yilbas BS. Effect of mud drying temperature on surface characteristics of a polycarbonate PV protective cover. Sol Energy 2017;143:63–72.
[43] Naghavi MS. Experimental and numerical assessments of underlying natural air movement on PV modules temperature. Sol Energy 2021;216:610–22.
[44] Abdullah Abdullah A. Effect of cooling method on the performance of PV/Trombe wall: experimental assessment. Therm Sci Eng Prog 2022;30:101273.
[45] Saad M, Saidur R, Kamalisarvestani M. Effect of dust, humidity and air velocity on efficiency of photovoltaic cells. Renew Sustain Energy Rev 2012;16(5):2920–5.
[46] Gökmen Nuri. Investigation of wind speed cooling effect on PV panels in windy locations. Renew Energy 2016;90:283–90.
[47] Elminshawy Nabil AS. Simulation and experimental performance analysis of partially floating PV system in windy conditions. Sol Energy 2021;230:1106–21.
[48] Tripathi Abhishek Kumar. Evaluation of solar PV panel performance under humid atmosphere. Mater Today Proc 2021;45:5916–20.
[49] Lawrence MG. The relationship between relative humidity and the Dewpoint temperature in moist air: a simple conversion and applications. Bull Am Meteorol Soc 2022;86:225–34.
[50] Bora Birinchi. Accelerated stress testing of potential induced degradation susceptibility of PV modules under different climatic conditions. Sol Energy 2021;223:158–67.
[51] Jin ho Choi. Power performance of high-density photovoltaic module using energy balance model under high humidity environment. Sol Energy 2021;219:50–7.
[52] Kaaya Ismail. Assessment of uncertainties and variations in PV modules degradation rates and lifetime predictions using physical models. Sol Energy 2021;218:354–67.
[53] Tan Cher Ming, Chen Boon Khai Eric, Toh Kok Peng. Humidity study of a-Si PV cell. Microelectron Reliab 2010;50:1871–4.
[54] Kazem Hussein A, Miqdam T Chaichan. Effect of humidity on photovoltaic performance based on experimental study. Int J Appl Eng Res 2015;10(23):43572–7.
[55] Andrews Rob W, Pollard Andrew, Pearce Joshua M. The effects of snowfall on solar photovoltaic performance. Sol Energy 2013;92:84–97.
[56] Pawluk Robert E, Chen Yuxiang, et al. Photovoltaic electricity generation loss due to snow–A literature review on influence factors, estimation, and mitigation. Renew Sustain Energy Rev 2019;107:171–82.
[57] Ghazi Sanaz, Kenneth Ip. The effect of weather conditions on the efficiency of PV panels in the southeast of UK. Renew Energy 2014;69:50–9.
[58] Heidari Negin. Impact of snow and ground interference on photovoltaic electric system performance. IEEE J Photovoltaics 2015;5(6):1680–5.
[59] Powers Loren, Newmiller Jeff, et al. Measuring and modeling the effect of snow on photovoltaic system performance. In: 2010 35th IEEE photovoltaic specialists conference. IEEE; 2010.
[60] Muehleisen Wolfgang. Outdoor detection and visualization of hailstorm damages of photovoltaic plants. Renew Energy 2018;118:138–45.
[61] Lillo-Bravo Isidoro. Impact of energy losses due to failures on photovoltaic plant energy balance. Energies 2018;11(2):363.
[62] Moser D, Del Buono M, Bresciani W, et al. Technical risks in PV projects development and PV plant operation D1.1. D2.1, vol. 1. Solar Bankability Project; 2016. p. 1–109.
[63] Gallardo-Saavedra S, Hernández-Callejo L, Alonso-García M del C, et al. Nondestructive characterization of solar PV cells defects by means of electroluminescence, infrared thermography, I–V curves and visual tests: experimental study and comparison. Energy 2020:117930.
[64] Osawa S, Nakano T, Matsumoto S, et al. Fault diagnosis of photovoltaic modules using AC impedance spectroscopy. In: Ieee Int. Conf. Renew. Energy Res. Appl. Brimingham, UK; 2016. p. 210–5.
[65] Simon M, Meyer EL. Detection and analysis of hot-spot formation in solar cells. Sol Energy Mater Sol Cells 2010;94:106–13.
[66] Laurino Marica, Piliougine Michel, et al. Artificial neural network based photovoltaic module diagnosis by current–voltage curve classification. Sol Energy 2022;236:383–92.
[67] Ma Mingyao. Fault diagnosis of PID in crystalline silicon photovoltaic modules through IV curve. Microelectron Reliab 2021;126:114236.
[68] Zhang Zhixiang. A fault diagnosis method for photovoltaic module current mismatch based on numerical analysis and statistics. Sol Energy 2021;225:221–36.
[69] Ma Mingyao. Fault diagnosis of cracks in crystalline silicon photovoltaic modules through IV curve. Microelectron Reliab 2020;114:113848 [Precise performance diagnosis of photovoltaic string by operation voltage and current: Experimental verification].
[70] Liu Yongjie. Intelligent fault diagnosis of photovoltaic array based on variable predictive models and I–V curves. Sol Energy 2022;237:340–51.
[71] Li Baojie. Fault diagnosis of photovoltaic panels using full I–V characteristics and machine learning techniques. Energy Convers Manag 2021;248:114785.
[72] Liu Yongjie. Fault diagnosis approach for photovoltaic array based on the stacked auto-encoder and clustering with IV curves. Energy Convers Manag 2021;245:114603.
[73] Oh Wonwook. Initial detection of potential-induced degradation using dark I–V characteristics of crystalline silicon photovoltaic modules in the outdoors. Microelectron Reliab 2018;88:998–1002.
[74] Seapan Manit. Detection of shading effect by using the current and voltage at maximum power point of crystalline silicon PV modules. Sol Energy 2020;211:1365–72.
[75] Zhang WJ, Ge Q, Huang CY. The research of photovoltaic array intelligent fault diagnosis based on the BP neural network. Adv Mater Res 2014;936:2201–6.
[76] Lu X, Lin P, Cheng S, et al. Fault diagnosis for photovoltaic array based on convolutional neural network and electrical time series graph. Energy Convers Manag 2019;196:950–65.
[77] Manohar M, Koley E, Ghosh S. Enhancing the reliability of protection scheme for PV integrated microgrid by discriminating between array faults and symmetrical line faults using sparse auto encoder. IET Renew Power Gener 2019;13:308–17.
[78] Chen Z, Chen Y, Wu L, et al. Deep residual network based fault detection and diagnosis of photovoltaic arrays using current-voltage curves and ambient conditions. Energy Convers Manag 2019;198:111793.
[79] Hopwood MW, Gunda T, Seigneur H, et al. Neural network-based classification of string-level IV curves from physically-induced failures of photovoltaic modules. IEEE Access 2020;8:161480–7.
[80] International Electrotechnical Commission (IEC) 61646. Thin-film terrestrial photovoltaic modules-Design qualification and type approval. 2008.
[81] International Electrotechnical Commission (IEC) 61215. Crystalline silicon terrestrial photovoltaic (PV) modules-design qualification and type approval. 2005.
[82] Bouraiou A, Hamouda M, Chaker A, et al. Experimental investigation of observed defects in crystalline silicon PV modules under outdoor hot dry climatic conditions in Algeria. Sol Energy 2018;159:475–87.
[83] Ahmed Faris Amiri, Oudira Houcine, Chouder Aissa, et al. Faults detection and diagnosis of PV systems based on machine learning approach using random forest classifier. Energy Convers Manag 2024;301:118076. Feb.
[84] Bouaichi A, Alami A, El A, et al. Experimental evaluation of the discoloration effect on PV-modules performance drop. Energy Proc 2017;119:818–27.
[85] Kahoul N, Chenni R, Cheghib H, et al. Evaluating the reliability of crystalline silicon photovoltaic modules in harsh environment. Renew Energy 2017;109:66–72.
[86] Bouraiou A, Hamouda M, Chaker A, et al. Experimental evaluation of the performance and degradation of single crystalline silicon photovoltaic modules in the Saharan environment. Energy 2017;132:22–30.
[87] Li X, Wang J, Yang Q, et al. Intelligent fault pattern recognition of aerial photovoltaic module images based on deep learning technique. In: Proc. Complexity, Informatics and Cybernetics; 2017. Orlando, Florida, USA, August.
[88] Li X, Yang Q, Chen Z, et al. Visible defects assessment based on UAV imaging analysis for large-scale photovoltaic systems. IET Renewable Power Generation, Spec. Performance assessment and condition monitoring of photovoltaic systems for improved energy yield 2017;11(10):1234–44. September.
[89] Gallardo-Saavedra S, Hernández-Callejo L, Duque-Pérez A. Analysis and characterization of PV module defects by thermographic inspection. Rev Fac Ing 2019;(93):92–104.
[90] Á.H. Herraiz, A.P. Marugán, F.P.G. Márquez, Chapter 7 - a review on condition monitoring system for solar plants based on thermography.
[91] Papaelias M, Márquez FPG, Karyotakis A, editors. Non-destructive Testing and condition monitoring techniques for renewable energy industrial Assets. Boston: Butterworth-Heinemann; 2020. p. 103–18.

[92] Haidari Parsa, et al. Deep learning-based model for fault classification in solar modules using infrared images. Sustain Energy Technol Assessments 2022;52:102110.
[93] Wang Xing, et al. Intelligent monitoring of photovoltaic panels based on infrared detection. Energy Rep 2022;8:5005–15.
[94] Shen Yu. Modified U-Net based photovoltaic array extraction from complex scene in aerial infrared thermal imagery. Sol Energy 2022;240:90–103.
[95] Akram M Waqar. Automatic detection of photovoltaic module defects in infrared images with isolated and develop-model transfer deep learning. Sol Energy 2020;198:175–86.
[96] Zefri Yahya. Developing a deep learning-based layer-3 solution for thermal infrared large-scale photovoltaic module inspection from orthorectified big UAV imagery data. Int J Appl Earth Obs Geoinf 2022;106:102652.
[97] Ali Muhammad Umair. A machine learning framework to identify the hotspot in photovoltaic module using infrared thermography. Sol Energy 2020;208:643–51.
[98] Alves Ricardo Henrique Fonseca, et al. Automatic fault classification in photovoltaic modules using Convolutional Neural Networks. Renew Energy 2021;179:502–16.
[99] Su B, Chen H, Liu K, et al. RCAG-net: residual Channelwise attention gate network for hot spot defect detection of photovoltaic farms. IEEE Trans Instrum Meas 2021;70:1–14.
[100] Cavieres Robinson. Automatic soiling and partial shading assessment on PV modules through RGB images analysis. Appl Energy 2022;306:117964.
[101] Espinosa Alejandro Rico, Bressan Michael, et al. Failure signature classification in solar photovoltaic plants using RGB images and convolutional neural networks. Renew Energy 2020;162:249–56.
[102] Li X, Li W, Yang Q, Yan W, Zomaya AY. Edge-Computing-Enabled Unmanned Module Defect Detection and Diagnosis System for Large-Scale Photovoltaic Plants," in. IEEE Inter Thing J Oct. 2020;7(10):9651–63.
[103] Li X, Yang Q, Yan W. Deep learning-based module defect analysis for large-scale photovoltaic farms. IEEE Trans Energy Convers 2019;34(1):520–9. March.
[104] Hong Feng. A novel framework on intelligent detection for module defects of PV plant combining the visible and infrared images. Sol Energy 2022;236:406–16.
[105] Di Tommaso Antonio, Betti Alessandro, Fontanelli Giacomo, Michelozzi Benedetto. A multi-stage model based on YOLOv3 for defect detection in PV panels based on IR and visible imaging by unmanned aerial vehicle. Renew Energy 2022;193:941–62.
[106] Oliveira de, Aline Kirsten Vidal, Aghaei Mohammadreza. Aerial infrared thermography for low-cost and fast fault detection in utility-scale PV power plants. Sol Energy 2020;211:712–24.
[107] Jahn U, Herz M, Köntges M. Review on infrared and electroluminescence imaging for PV field applications. IEA-PVPS T13-10:2018: Tech. rep. International Energy Agency Photovoltaic Power Systems Programme 2018:100.
[108] Zhao Shenshen, Chen Haiyong, Wang Chuhan, et al. RGR-Net: Refined Graph Reasoning Network for multi-height hotspot defect detection in photovoltaic farms. Expert Syst Appl 2024;245:123034. Feb.
[109] Kuo Chung-Feng Jeffrey, Chen Sung-Hua, et al. Automatic detection, classification and localization of defects in large photovoltaic plants using unmanned aerial vehicles (UAV) based infrared (IR) and RGB imaging. Energy Convers Manag 2024;276:116495. Jan.
[110] Sun Tianyi, Xing Huishuang, Cao Shengxian, et al. A novel detection method for hot spots of photovoltaic (PV) panels using improved anchors and prediction heads of YOLOv5 network. Energy Rep 2022;8:1219–29. Nov.
[111] Ghosh Swatilekha, Singh Santosh Kumar, Kumar Yadav Vinod. Experimental investigation of hotspot phenomenon in PV arrays under mismatch conditions. Sol Energy 2023;253:219–30. Mar.
[112] W. Tang, Q. Yang, X. Hu, "Edge intelligence for smart EL images defects detection of PV plants in the IoT-based inspection system," IEEE Internet Things J, doi: 10.1109/JIOT.2022.3150298.
[113] Photovoltaic devices - Part 13: Electroluminescence of photovoltaic modules, International Electrotechnical Commission, Geneva, CH (2018).
[114] Tang Wuqin, Yang Qiang, Hu Xiaochen, Yan Wenjun. Convolution neural network based polycrystalline silicon photovoltaic cell linear defect diagnosis using electroluminescence images. Expert Syst Appl 2022;202:117087.
[115] dos Reis Benatto GA, Riedel N. Development of outdoor luminescence imaging for drone-based PV array inspection. In: The 44th IEEE photovoltaic specialists conference (PVSC). Washington, DC: IEEE; 2017. p. 2682–7.
[116] Kropp T, Berner M, Stoicescu L. Self-sourced daylight electroluminescence from photovoltaic modules. IEEE J Photovolt 2017;7(5):1184–9.
[117] Parikh HR, Spataru S, Sera D. A photovoltaic module diagnostic setup for lock-in electroluminescence imaging. In: Proceedings of 46th IEEE photovoltaic specialists conference (PVSC). Chicago, IL: IEEE; 2019. p. 538–43.
[118] Tang W, Yang Q, Yan W. Deep Learning-Based Algorithm for Multi-Type Defects Detection in Solar Cells with Aerial EL Images for Photovoltaic Plants. CMES-Comput Model Eng Sci 2022;130(3):1423–39.
[119] Tang W, Yang Q, Yan W, et al. Deep learning based automatic defect identification of photovoltaic module using electroluminescence images. Sol Energy 2020;201(C):453–60.
[120] Akram MW, Li G, Jin Y, X, et al. CNN based automatic detection of photovoltaic cell defects in electroluminescence images. Energy 2019. https://doi.org/10.1016/j.energy.2019.116319.
[121] Islam MA, Hasanuzzaman M, Rahim NA. Investigation of the potential induced degradation of on-site aged polycrystalline PV modules operating in Malaysia. Measurement 2018;119:283–94.
[122] Sergiu D, Vincent C, Stephan B, et al. Automatic classification of defective photovoltaic module cells in electroluminescence images. Sol Energy 2019;185:455–68.
[123] French R, Karimi A, Braid J. EL-cell-images-single-brand-dampheat. 2019. Dec.
[124] Lawrence P, Devashen G, Richard K. Defect detection and quantification in electroluminescence images of solar PV modules using U-net semantic segmentation. Renew Energy 2021;178:1211–22.
[125] Ahmad M, Justin S, Nicholas A, et al. Generalized and Mechanistic PV module performance prediction from computer vision and machine learning on electroluminescence images. IEEE J Photovoltaics 2020;10(3):878–87.
[126] Wang Youyang, Li Liying, Sun Yifan, et al. Adaptive automatic solar cell defect detection and classification based on absolute electroluminescence imaging. Energy 2021;229:120606.
[127] Zhang Xiong, Yawen Hao, Shangguan Hong, et al. Detection of surface defects on solar cells by fusing Multi-channel convolution neural networks. Infrared Phys Technol 2020;108:103334.
[128] Rahman Muhammad Rameez Ur, Chen Haiyong. Defects inspection in polycrystalline solar cells electroluminescence images using deep learning. IEEE Access 2020;8:40547–58.
[129] Lin Keh-Moh, Lin Horng-Horng, Lin You-The. Development of a CNN-based hierarchical inspection system for detecting defects on electroluminescence images of single-crystal silicon photovoltaic modules. Mater Today Commun 2022:103796.
[130] Urtzi O, Ingo M, Marco Q, et al. Segmentation of cell-level anomalies in electroluminescence images of photovoltaic modules. Sol Energy 2021;220:914–26.
[131] Mustafa D, Nurettin B, Abdülkadir G. Efficient deep feature extraction and classification for identifying defective photovoltaic module cells in Electroluminescence images. Expert Syst Appl 2021;175:114810.
[132] Ahmad M, Justin S, Mohammad A, et al. Automated pipeline for photovoltaic module electroluminescence image processing and degradation feature classification. IEEE J Photovoltaics 2019;9(5):1324–35.
[133] Mahmoud D, Violeta H. Solar cells micro crack detection technique using state-of-the-art electroluminescence imaging. J Sci: Advanced Materials and Devices 2019;4(4):499–508.
[134] Ge C, Liu Z, Fang L, et al. A hybrid Fuzzy convolutional neural network based mechanism for photovoltaic cell defect detection with electroluminescence images. IEEE Trans Parallel Distr Syst 2020;(99):1653–64.
[135] Tang W, Yang Q, Hu X, Yan W. Deep learning-based linear defects detection system for large-scale photovoltaic plants based on an edge-cloud computing infrastructure. Sol Energy 2021;231:527–35. Nov.
[136] Pratt Lawrence, Mattheus Jana, Klein Richard. A benchmark dataset for defect detection and classification in electroluminescence images of PV modules using semantic segmentation. Systems and Soft Computing 2023;5.
[137] Liu Qing, Liu Min, Wang Chenze, et al. An efficient CNN-based detector for photovoltaic module cells defect detection in electroluminescence images. Sol Energy 2024;267:112245.
[138] Yousif Hayder, Al-Milaji Zahraa. Fault detection from PV images using hybrid deep learning model. Sol Energy 2024;267:112207. Jan.
[139] Zhang Jinxia, Chen Xinyi, Wei Haikun. A lightweight network for photovoltaic cell defect detection in electroluminescence images based on neural architecture search and knowledge distillation. Appl Energy 2024;355:122184. Feb.
[140] Cao Yukang, Pang Dandan, Zhao Qianchuan, et al. A Improved YOLOv8-GD deep learning model for defect detection in electroluminescence images of solar photovoltaic modules. Eng Appl Artif Intell 2024;131:107866. May.
[141] Xie Xiangying, Lai Guangzhi, You Meiyue. Effective transfer learning of defect detection for photovoltaic module cells in electroluminescence images. Sol Energy 2023;250:312–23. Jan.
[142] Bhoopathy R, Kunz O, Juhl M. Outdoor photoluminescence imaging of photovoltaic modules with sunlight excitation. Wiley Progr Photovolt 2018;26:69–73.
[143] dos RGA, Chi M, Jensen OB, et al. Photoluminescence imaging induced by laser line scan: study for outdoor field inspections. In: IEEE 7th world conference on photovoltaic energy conversion. IEEE; 2018. p. 395–9.
[144] Kasemann M, Reindl LM, Michl B, et al. Contactless qualitative series resistance imaging on solar cells. IEEE J Photovolt 2012;2(2):181–3.
[145] dos RGA, Santamaria LAA, Hass TK, et al. Detection of solar cell cracks by laser line induced lateral currents and luminescence imaging. In: 37th European photovoltaic solar energy conference and exhibition. EUPVSEC; 2020. p. 1053–7.
[146] Silverman TJ, Deceglie MG, VanSant K. Illuminated outdoor luminescence imaging of photovoltaic modules. In: 2017 IEEE 44th photovoltaic Specialist conference (PVSC); 2017. p. 3452–5.
[147] Adhya S, Saha D, Das A, et al. An IoT based smart solar photovoltaic remote monitoring and control unit. In: 2016 2nd IEEE international conference on control, instrumentation, energy & communication; 2016. p. 432–6.
[148] Shrihariprasath B, Rathinasabapathy V. A smart IoT system for monitoring solar PV power conditioning unit. In: IEEE world conference on futuristic trends in research and innovation for social welfare; 2016. p. 1–5.
[149] Sheikh AR, Tania U, David AP. PV system defects identification using Remotely Piloted Aircraft (RPA) based infrared (IR) imaging: a review. Sol Energy 2020;206:579–95.
[150] Isaac SR, Jesús RC, Fausto PG. Unmanned aerial vehicle integrated real time kinematic in infrared inspection of photovoltaic panels. measurement 2022;188:110536.

[151] Moradi Sizkouhi AM, Esmailifar SM, Aghaei M, et al. RoboPV: an integrated software package for autonomous aerial monitoring of large scale PV plants. Energy Convers Manag 2022;254:115217.

[152] Isaac S.R., Alberto P.M., Fausto P.M., "A novel approach to optimize the positioning and measurement parameters in photovoltaic aerial inspections," Renew Energy, 187:371-389.

[153] Vergura S. Correct settings of a Joint unmanned aerial vehicle and infrared camera system for the detection of faulty photovoltaic modules. IEEE J Photovoltaics 2021;11(1):124–30. Jan.